

GBT Rolling Weight Measurements  
methods, results, estimation of uncertainty,  
and auxiliary measurements

David H. Parker

Robert Anderson

Dennis Egan

Troy Fakes

Bill Radcliff

John Shelton

October 23, 2003

# Contents

<b>1</b>	<b>Introduction</b>	<b>1</b>
1.1	Outline of Methods . . . . .	1
1.2	Equipment . . . . .	1
<b>2</b>	<b>Execution of Measurements</b>	<b>4</b>
2.1	Initial Load Cell Calibration . . . . .	4
2.2	Procedures . . . . .	4
2.2.1	mechanical . . . . .	4
2.2.2	instrumentation and data collection . . . . .	7
2.2.3	cell loading . . . . .	7
2.2.4	schedule . . . . .	12
2.2.5	included weight . . . . .	12
2.3	Follow-up Load Cell Calibration . . . . .	15
<b>3</b>	<b>Results</b>	<b>17</b>
3.1	Treatment of Data . . . . .	17
3.2	Calculated Weights . . . . .	22
3.3	Estimation of Uncertainty . . . . .	22
<b>4</b>	<b>Auxiliary Measurements</b>	<b>24</b>
4.1	Jack Stroke Measurements . . . . .	24
4.2	Wheel Housing-to-Wiffle Beam . . . . .	24
4.2.1	wheel 13 . . . . .	25
4.3	Horizontal Deflection of Wiffle Beam . . . . .	25
4.4	Flex Plate Length Measurements . . . . .	30
4.5	Idler Wheel Movement . . . . .	32
4.6	Pointer Readings . . . . .	32
<b>5</b>	<b>Summary</b>	<b>34</b>
5.1	Notes on Appendices . . . . .	34
5.2	Acknowledgments . . . . .	34
<b>A</b>	<b>Options and Methods for Weighing the GBT</b>	<b>I</b>
<b>B</b>	<b>Proposed Procedure for Weighing the GBT</b>	<b>II</b>
<b>C</b>	<b>Geokon Load Cell Manual</b>	<b>III</b>
<b>D</b>	<b>Pressure Gage Calibration Reports</b>	<b>IV</b>
<b>E</b>	<b>Jack and Hydraulic Drawings</b>	<b>V</b>
<b>F</b>	<b>Pre-weighing Calibration</b>	<b>VI</b>
<b>G</b>	<b>Load Field Notes and Location Sketches</b>	<b>VII</b>

<b>H</b>	<b>Pointer Field Notes</b>	<b>VIII</b>
<b>I</b>	<b>Inclinometer Field Notes</b>	<b>IX</b>
<b>J</b>	<b>Post-weighing Calibration</b>	<b>X</b>
<b>K</b>	<b>Force, Angle, and Excitation Plots</b>	<b>XI</b>
<b>L</b>	<b>Force Tables—Load Cells</b>	<b>XII</b>
<b>M</b>	<b>Force Tables—Hydraulic Jacks</b>	<b>XIII</b>
<b>N</b>	<b>Indicator Plots</b>	<b>XIV</b>
<b>O</b>	<b>CD</b>	<b>XV</b>
	O.1 Calibration Reports and Photos . . . . .	XV
	O.2 Excel files . . . . .	XV
	O.3 Photos . . . . .	XV
	O.4 $\text{\TeX}$ Files . . . . .	XV
	O.5 Powerpoint File . . . . .	XV

# List of Figures

1.1	The Robert C. Byrd Green Bank Telescope. . . . .	2
1.2	Geokon 2,000 kip load cell. . . . .	2
2.1	Materials testing machine and platens. . . . .	5
2.2	Load cell centered on platens with aluminum plates. . . . .	5
2.3	Load cell between platens. . . . .	6
2.4	Alidade corner . . . . .	6
2.5	N3 Optical level . . . . .	8
2.6	Clineometer measurement of corner weldment . . . . .	9
2.7	Instrumentation truck. . . . .	9
2.8	End view of wiffle beam. . . . .	10
2.9	Initial load cell configuration. . . . .	10
2.10	Revised load cell configuration. . . . .	11
2.11	Inboard lifting fixture. . . . .	12
2.12	Hydraulic system. . . . .	13
2.13	Schedule of Operations. . . . .	13
2.14	Crew. . . . .	14
2.15	Load cell calibration with lead sheets. . . . .	15
3.1	Histogram of ascending $\Delta F/\Delta\alpha$ for load cells. . . . .	18
3.2	Histogram of descending $\Delta F/\Delta\alpha$ for load cells. . . . .	18
3.3	Histogram of ascending $\Delta F/\Delta\alpha$ for hydraulic pressure. . . . .	19
3.4	Histogram of descending $\Delta F/\Delta\alpha$ for hydraulic pressure. . . . .	19
3.5	Histograms of residual load cell force on cell 1976—including jack friction. . . . .	20
3.6	Histograms of residual load cell force on cell 2081—including jack friction. . . . .	20
3.7	Histograms of zero force on cell 1976. . . . .	21
3.8	Histograms of zero force on cell 2081. . . . .	21
3.9	Summary of GBT rolling weight. . . . .	22
4.1	Typical jack stroke measurement data . . . . .	25
4.2	Measurement of vertical motion between wheel housing and wiffle beam . . . . .	26
4.3	Vertical movement between wheel housing and wiffle beam—jacking beam. . . . .	27
4.4	Vertical movement between wheel housing and wiffle beam—idler beam. . . . .	27
4.5	Measurement of vertical motion between wheel housing and wiffle beam at both distal flex plates. . . . .	28
4.6	Measurement of vertical motion between wheel housing and wiffle beam at both proximal flex plates. . . . .	28
4.7	Measurement of horizontal deflection of wiffle beam. . . . .	29
4.8	Measurement of the compression of the top beams. . . . .	29
4.9	Flex plate length measurement. . . . .	30
4.10	Detail of flex plate length measurement. . . . .	31
4.11	Flex plate length data. . . . .	31
4.12	Idler circumferential measurement. . . . .	32
4.13	Idler wheel movement. . . . .	33

4.14 Table of pointer measurements . . . . .	33
--	----

## Abstract

Problems with the GBT track and wheels, inflation of the estimated weight over the course of the project, and questions about the design safety margins raised concerns about the accuracy of the estimated GBT rolling weight. At the outset of the project (and the basis for the track and wheel design), the rolling weight was estimated to be 12 030 kips (1000 lbf/kip)[1] (5 280 alidade, 6 750 tipping structure). The final estimated rolling weight was 16 159 kips[3] (5 465 alidade, 10 694 tipping structure), with no estimate of the uncertainty or asymmetry of the wheel load distribution.

A program was initiated[11], in January, 2003, to weigh each wiffle beam (wheel pair) of the GBT rolling structure with the goal of a relative combined standard uncertainty of less than 1%. This was conducted between March 17 and April 9, 2003, in 13 measurements—with one repeat due to wind; repeats of the first three measurements in order to incorporate improvements in methods gained with experience; and a repeat with the revised method to check the reproducibility of the methods. The measured weight was 16 727 kips with a combined standard uncertainty (level of confidence  $\approx 68\%$ ) of  $\pm 48$  kips, or a relative combined standard uncertainty of 0.3%. Two measurements of wheel pair 7 & 8, conducted on 3/24 and 4/8, reproduced within 5.5 kips, or 0.3%. To put this in perspective, a loaded 100 ton coal car weighs about 264 000 lbf—so the GBT weight is equivalent to  $63.3 \pm 0.2$  loaded coal cars.

While the total weight was only 3.5% higher than the final estimate[3] of 16,159 kips, no estimate had previously been made on the distribution of the load, i.e., it was assumed to be evenly distributed over the 16 wheels. The measured weight distribution revealed a maximum wiffle beam load (2 wheels) of 2199  $\pm$  10 kips, or 46% greater than the original wheel and track design assumptions and nearly 9% greater than the final symmetric load estimation.

In conjunction with lifting the wiffle beams, auxiliary measurements were made to capture additional data related to the wheel suspension system, flex plates, and wheel alignment.

This technical report, along with the appendices and references, memorializes the experimental data and methods used to: calibrate the instrumentation, weigh the telescope, and process the data. Due to the novel nature of the measurements, considerable detail is devoted to the methods, subtleties, and suggested improvements for similar projects. Due to the volume of the appendices (several hundred pages), they are only included in the GBT Archive file A0335.

# Chapter 1

## Introduction

### 1.1 Outline of Methods

At the outset of the project, a study was conducted to determine the availability of government lab and rental instrumentation, how accurately it could be calibrated, mechanical dimensions, telescope clearances, rental fee structures, etc. It became apparent that 2,000 kip (1000 ton) hydraulic jacks were readily available, but anything greater than that would probably have to be custom built and would not be available for rent. Two, 2,000 kip strain gage load cells were also available from the jack vendor; and while the vendor's calibration was not traceable to NIST, several capable calibration labs were identified that could provide certification at a reasonable fee[10].

Constraints on the clearance between adjacent waffle beams (see Figure 2.11) made it impractical to lift both waffle beams (required to lift a complete corner) with the existing fixturing provided by the GBT contractor and previously used to align the wheels and replace wheel bearings. Rather than getting into a redesign of the lifting fixturing, it was decided to lift one waffle beam at a time, i.e., 8 total lifts. This introduces a potential measurement error due to the torsional load introduced into the corner weldment and alidade. This is further complicated by the contractor's specification limiting the differential height between the waffle beam spherical bearings to 0.12 inches, i.e., a twist of the corner weldment of  $\approx 104$  seconds. A scheme was devised to measure the load as a function of lift height—and thus, under the assumption that small deflections are linear, extrapolate back to the load at zero height. For a more detailed report on various options and methods that were explored, see memo A0325[11].

### 1.2 Equipment

A search of the Thomas Register turned up Richard Dudgeon, Inc., Bridgeport, CT.(<http://dudgeonjacks.com>), as a good source for renting high capacity jacks. The Dudgeon 1000 ton (2000 kip) at 10 000 PSI, 2 inch stroke jack collapsed height is 6.6 inches with a 20.0 inch diameter footing and 16.0 inch diameter piston. This is a good match to the 19 inch wide ground and hardened GBT track wear strip, but the height is a little tight with the load cell stack and existing lifting fixtures. A few more inches of clearance with some filler plates would have been much better.

Sheet lead was used between the jack and load cell to insure a uniform load distribution on the load cell. The close fit, combined with gravity retraction of the jack (which had to be forced down by hand to create clearance), required a lot of work to remove the jack and deformed lead. For any future lifts, using these jacks and load cells, the fixtures should be shortened and provisions should be made to fully retract the jacks by a mechanical means. Three jacks were supplied (two for the measurements with a spare), as well as a 10 000 PSIG pump, manifold, and two calibrated pressure gages.

NIST has four 3,000 kip load cells, but they are 33 inches tall, heavy, and it would have probably required some political influence to persuade them to let them out of the lab. The US Army Primary Standards Lab at Redstone does not have any load cells in the required range. The standards lab at Marshall Space Flight Center located one 2,000 kip load cell at Kennedy Space Center, but of course we needed two. Fortunately, Dudgeon also has two 2 000 000 lbf compression load cells, but the calibrations

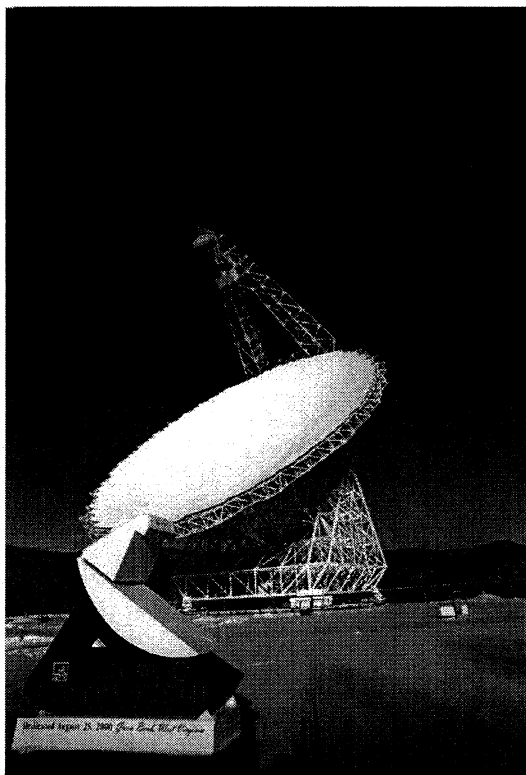


Figure 1.1: The Robert C. Byrd Green Bank Telescope.

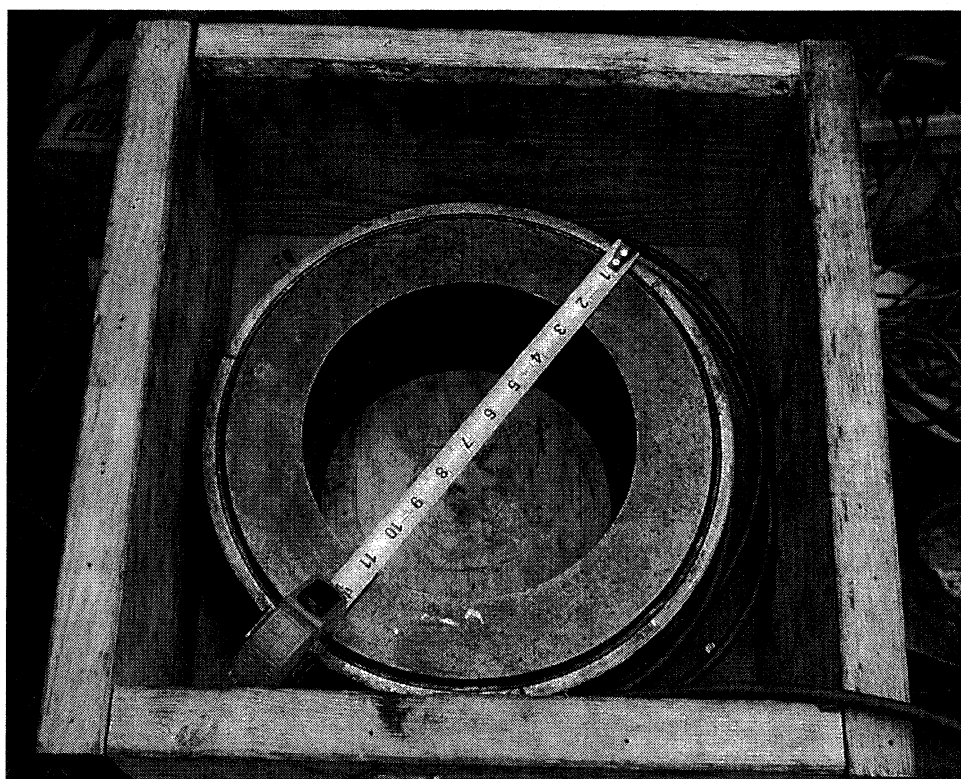


Figure 1.2: Geokon 2,000 kip load cell.

were questionable for the accuracy we required. These Series 3000 cells are built by Geokon Inc., Lebanon, NH (<http://www.geokon.com/>). They are strain gage instruments built on a 12.5 inch OD x 8.5 inch ID x 6.0 inch high cylinder, as shown in Figure 1.2. We rented the cells from Dudgeon and took responsibility for the calibration.

In order to insure absolute traceability of the load cells and instrumentation, an HP 3458A, 8.5 digit multimeter was rented from Instrument Rental Labs, Broomfield, CO, for the project. The instrument was last calibrated on 4/30/02, in its two year cycle, and they conduct a routine check before each rental. This instrument has a resolution of 0.01 microvolts and an uncertainty of 5 ppm. In order to filter line frequency noise, it uses an integrating A/D converter which integrates over integer periods of the line frequency. Using an integration over 90 cycles (1.5 s), the electronics noise was well under 0.1 microvolt.

## Chapter 2

# Execution of Measurements

### 2.1 Initial Load Cell Calibration

Prior to weighing, the load cells were calibrated by Dr. James W. Phillips, and associates, at the University of Illinois at Urbana-Champaign, Department of Theoretical and Applied Mechanics (<http://www.tam.uiuc.edu/directory/services/testing/facility.html>), on a 3,000 kip universal testing machine—which is traceable to NIST through their own load cell, which was calibrated by NIST in 2002. Both cells were calibrated on March 4, 2003 over the full 2,000 kip load, as per ASTM E-74, which requires that the cell be checked in three, 120 degree rotation orientations, over 11 equally spaced loads for a total of 33 test points at 11 load conditions. They were calibrated with the NRAO supplied HP 3458A multimeter in mV/V. The complete calibration report is included in Appendix F.

In general, the load cells were within specification, repeatable, and linear above 200 kips. The maximum deviations from linearity, over 200-2000 kips, were 0.1% and 0.05% of full load—or a maximum of 2 kips. The calibration lab did note electronic noise on the HP 3458A of around 1 microvolt. This was probably due to shorter integration times than we used in the field, but 1 microvolt resolution is sufficient (the main reason for using the HP 3458A was to insure traceable instrument uncertainty of better than 1 microvolt).

One precaution Geokon and the calibration labs stress when using a short, cylindrical load cell is to insure a repeatable and uniform load on the ends of the cell. This is covered in more detail in Appendix C (which unfortunately we did not see until the load cells arrived), and the literature. This was not fully appreciated initially, and the cells were loaded against 1/2 inch aluminum plates between the cell cylinder ends and the testing machine loading platens—primarily to protect the platens.

### 2.2 Procedures

#### 2.2.1 mechanical

The initial procedure was outlined in report A0325[11]. The telescope was placed at the survival elevation in order to minimize wind loading. All measurements were made at the same approximate azimuth in order to cancel possible prevailing wind induced moments from the total weight. At 10 mph, the maximum error/corner due to the moment about the elevation axis; moment about the cross elevation axis; drag force; and side force; were estimated to be: 6.6 kips, 9.3 kips, 3.4 kips, and 1 kip[11].

Each corner of the alidade is supported on a rigid corner weldment which rest on two pairs of spherical bearings, as shown in Figure 2.4. Each pair of spherical bearings,  $\approx 6.4$  feet apart in the radial direction, rest on waffle beams,  $\approx 20.1$  feet apart in the circumferential direction, with two wheels mounted in a flex plate suspension system (4 flex plates/wheel). The spherical bearing arrangement allows a wheel pair to pivot slightly about the telescope track radial direction in order to compensate for track irregularities. Since it was not practical to lift the entire corner, each waffle beam was weighed independently. While not as ideal as knife edges—to first order, the friction of the spherical bearings was assumed to be negligible, i.e., the combined load of the two load cells was equal to the vertical load on the spherical bearing pair.

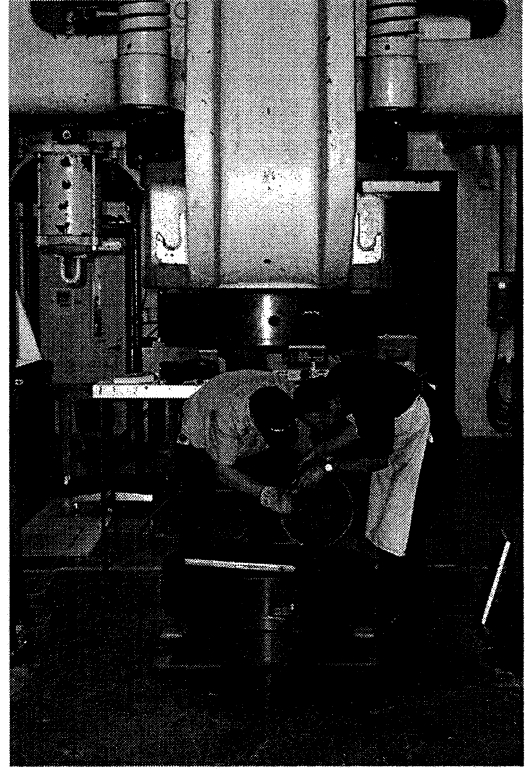
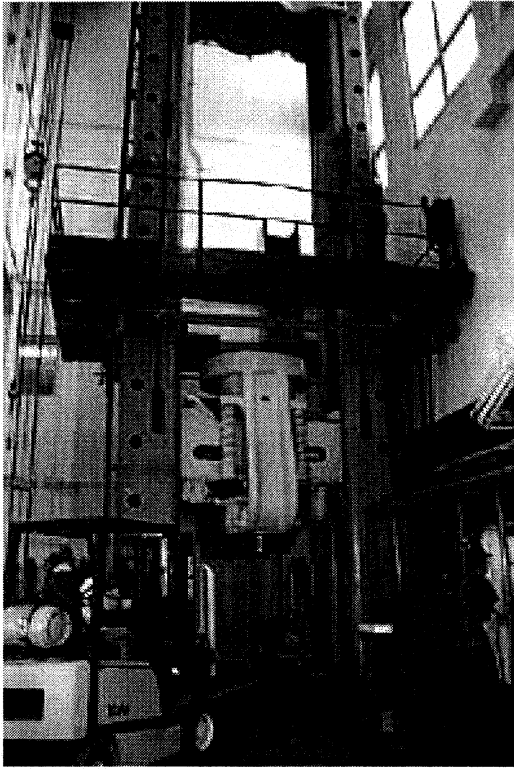


Figure 2.1: Materials testing machine and platens.



Figure 2.2: Load cell centered on platens with aluminum plates.

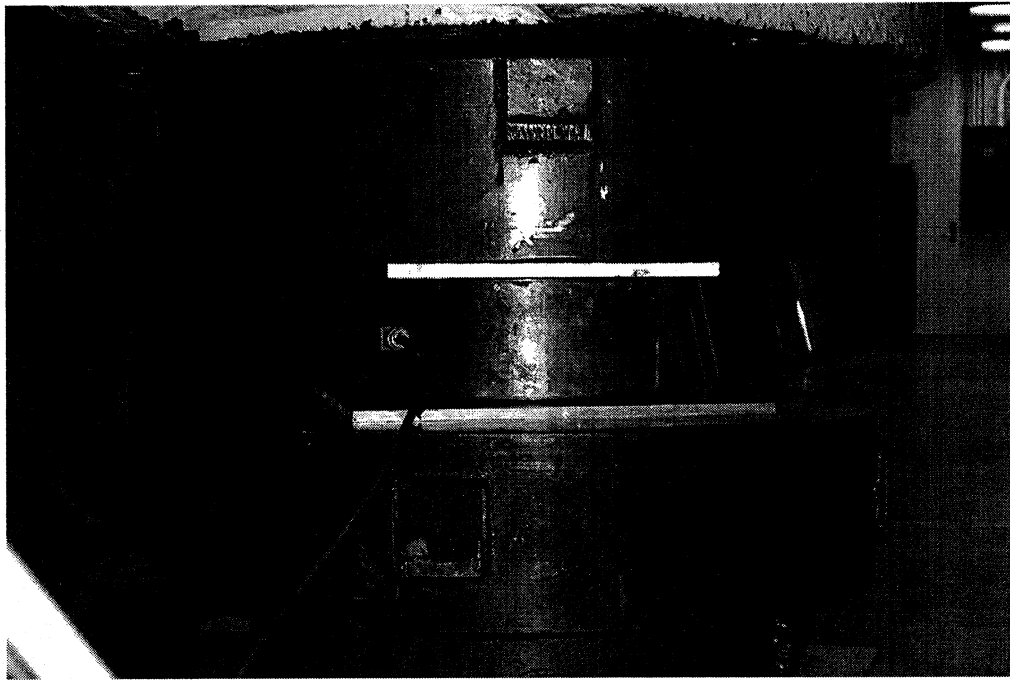


Figure 2.3: Load cell between platens.

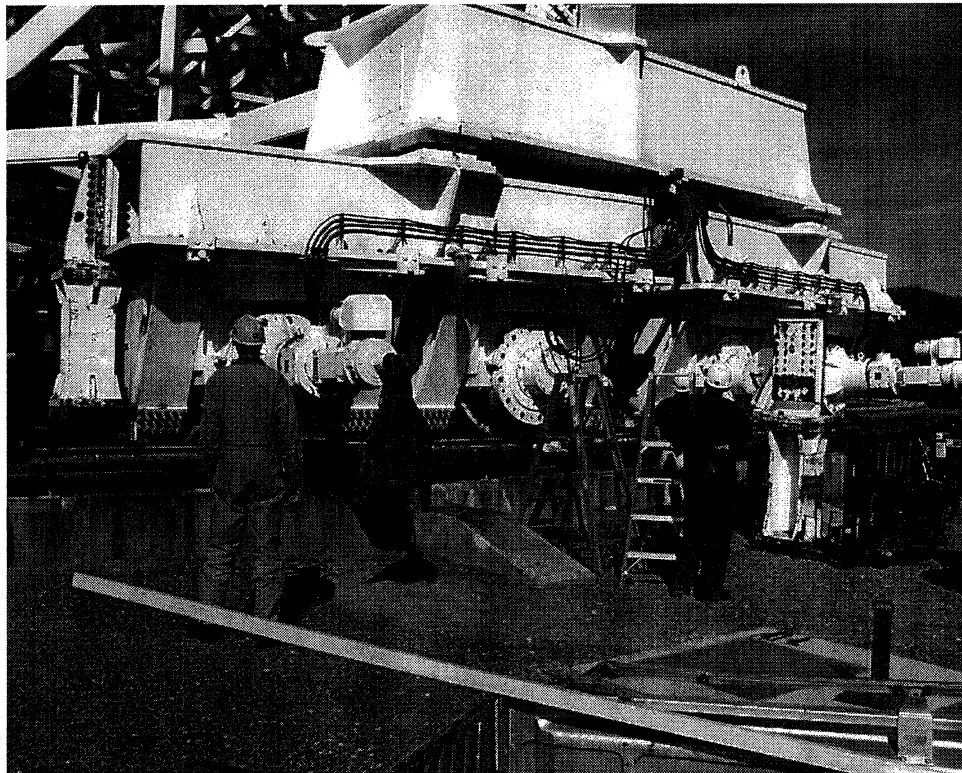


Figure 2.4: Alidade corner. Note waffle tree configuration of corner weldment, waffle beams, spherical bearings and lifting fixtures (one mounted on left end and one on ground near right end of waffle beam).

The lifting fixtures were approximately symmetric about the spherical bearings, so the loads were approximately equal. Since the jacks were located outside the wheels, and thus on a longer moment arm about the spherical bearings, care was taken to insure that both jacks always worked together in order to prevent a possible shift of load to a wheel—which could exceed the static load. For example, the wheels are approximately 55 inches off the spherical bearing line, while the jacks are approximately 112 inches. For a 2000 kip load at the spherical bearings carried by a wheel on one side and a jack on the other, the load on the wheel would be approximately 1341 kips—instead of 1000 kips for both wheels on the track.

Cribbing was also placed to minimize the drop in the event of a catastrophic failure, e.g., a hydraulic hose rupture which could drop one end of a wiffle beam and greatly exceed the static load on the wheel, bearing, and suspension—possibly resulting in cascading failures. In order to minimize lateral forces on the load cells, the brakes on the passive wheels were released. Digital indicator measurements of the circumferential motions of the passive wheels confirmed slight motion, as expected.

### 2.2.2 instrumentation and data collection

A detailed data sheet was constructed, and a note taker was assigned, in order to insure all relevant data was collected. The note taker checked to insure that the load cell, jack, and pressure gage locations were as specified on the data sheet, by serial number. Each load cell was marked at 0, 120, and 240 degree orientations. Additional auxiliary measurement digital indicator data was collected via handheld computers.

In order to insure that the lift did not exceed the 0.12 inch differential height between the spherical bearings, two methods were initially used. Targets were suspended from the corner weldment at each end, and the center, and a rod was located on a bench mark, as shown in Figure 2.5. An N3 optical level was used to shoot the targets and thus monitor the differential heights. In addition, a split-bubble clineometer was placed on the corner weldment, as shown in Figure 2.6. The specification translates to a maximum rotation of  $\approx 104$  seconds. The passive end of the corner weldment did not change height, and the clineometer and N3 measurements were in close agreement. The clineometer proved to be simpler, so the N3 measurements were abandoned after the first lift.

All of the instrumentation, power supplies, and a desk for the note taker and multimeter reader were located in a van with space at the rear door for the load cells, as shown in Figure 2.7. In order to minimize warm-up time for the instrumentation, a UPS power supply was provided to maintain the instrumentation while moving between the lab and telescope, and the instrumentation was left powered up with the load cells connected from March 14–April 10. The truck was also parked outside in ambient conditions. The excitation sense and output Voltages (6 wire connection) were multiplexed through a manual switch to the multimeter which was set on an integration period of 90 power line cycles (1.5 s).

The note taker recorded the time; lift stage; excitation Voltages; hydraulic pressures; output Voltages; peak-to-peak signal (noise) level; a shorted input reading (instrument zero); and notes on the experiment; as they were called out to him. Between measurements, the note taker did a quick calculation of the individual, difference, and combined weights in order to check for blunders and the repeatability in the field. The inclinometer readings, time, and lift stage were recorded in a surveyor's field book. We were also concerned about the fact that the track and the face of the lifting fixtures were not exactly parallel, and assumed they change due to the distortion of the wiffle beam as the load shifted from the wheels to the lifting fixtures. We recorded the fixture angles with a digital level oriented parallel to both the radial and tangential directions under each condition. The wheel manufacturers pointer indications between the wiffle beam and wheel housing (used to measure twist of the flex plate suspension system) for both loaded and unloaded conditions were recorded. We also manually recorded the load cell temperatures with a contact thermometer, and the site weather was logged via computer.

Digital indicators were used to measure the change in height of each lifting fixture on the ends of the wiffle beam. While this is influenced by deflections in the track as the load shifts from the wheels to the jacks—and thus not accurate enough to measure the differential height of the spherical bearings—with experience they were useful to estimate when the wheels cleared the track and incremental changes.

### 2.2.3 cell loading

Due to the close fit between the track and lifting fixture, we could not use 1/2 inch aluminum plates on the ends of the load cells—as per the calibration conditions. The face of the jacks and lifting fixtures were

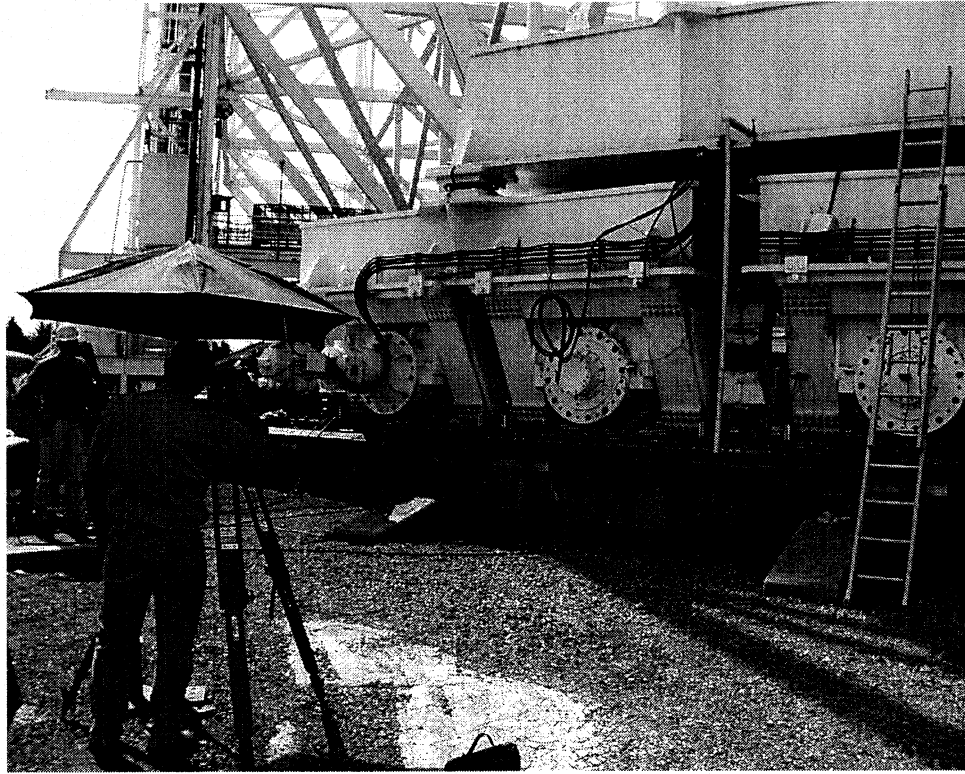


Figure 2.5: N3 optical level. Note temporary target clamped to center of corner weldment. See Figure 2.6 for view of a spherical bearing target.

relatively flat, but not a ground finish. We decided to use 1/16 inch thick sheet lead on the ends of the load cells in order to minimize the impact of surface finish and create more reproducible results.

Starting with wheels 1 & 2 (first pair of wheels CCW to the alidade stairs), on March 17, the initial configuration was track/jack/lead/load cell/lead/fixture, as shown in Figure 2.9. Each set of measurements were repeated at 0, 120, and 240 degree rotations of the load cell pair. The repeatability of the three orientations was not as good as in the calibration lab. One theory was that the load distribution on the fixture was not uniform. The fixture looks like an H beam with a 22 x 22 x 3 inch end plate, as shown in Figure 2.8. Unlike the much thicker materials testing machine platens (see Figure 2.3), or even the jack piston, which is backed up by the hydraulic fluid, the H shape could imprint through the 3 inch plate into the load on the cell. This was not detectable on pressure sensitive film that was used to do a qualitative check of the pressure distribution on the load cell ends, but the pattern was not totally symmetric.

Starting with wheel pairs 7 & 8, on March 24, fixturing was built to invert the jack against the lifting fixture and thus put the load cell between the track and jack piston, i.e., track/lead/load cell/lead/jack/fixture, as shown in Figure 2.10. When this was tried, we serendipitously discovered that when hydraulic oil leaked on the lead sheet, it flowed much more than dry lead. We also got more repeatable results on that run and the pressure sensitive film looked more uniform, so we thought the lubrication may have been beneficial. From that point on we lubricated the lead sheets with WD-40 and continued to use the inverted jack arrangement. We also discovered that we got more repeatable results by doing a pre-lift for each orientation. It should be pointed out that subsequent tests on the materials testing machine confirmed increased lead flow, but did not show a significant difference in the repeatability between dry and lubricated lead against the smooth platens. They did, however, show improvements in hysteresis by doing a preload to seat the lead.

The waffle beam was lifted until a shim stock sword could pass under each wheel. This usually required isolating one jack at the manifold, shown in Figure 2.12, for the last fine tuning if one wheel went slightly ahead of the other. This typically required about 0.35 inches of jack stroke to redistribute the load on the waffle beam and relieve the flex plate suspension, and produced a rotation of the corner weldment of around



Figure 2.6: Clineometer measurement of corner weldment twist. Note clineometer at top of ladder, and N3 target hanging directly under spherical bearings.

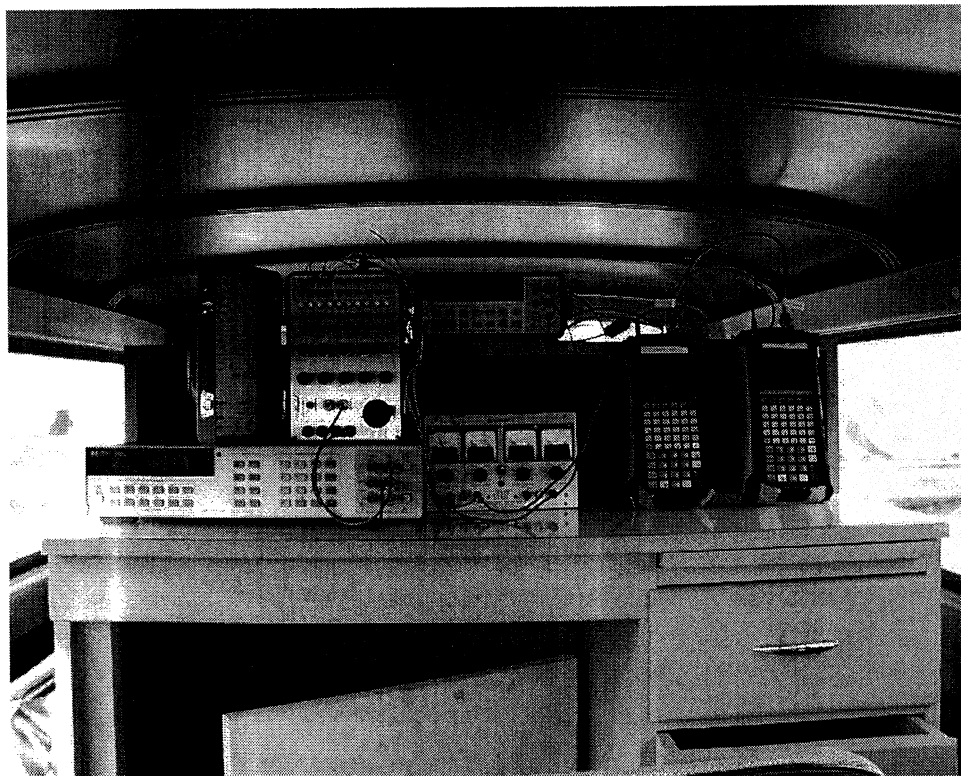


Figure 2.7: Instrumentation truck.

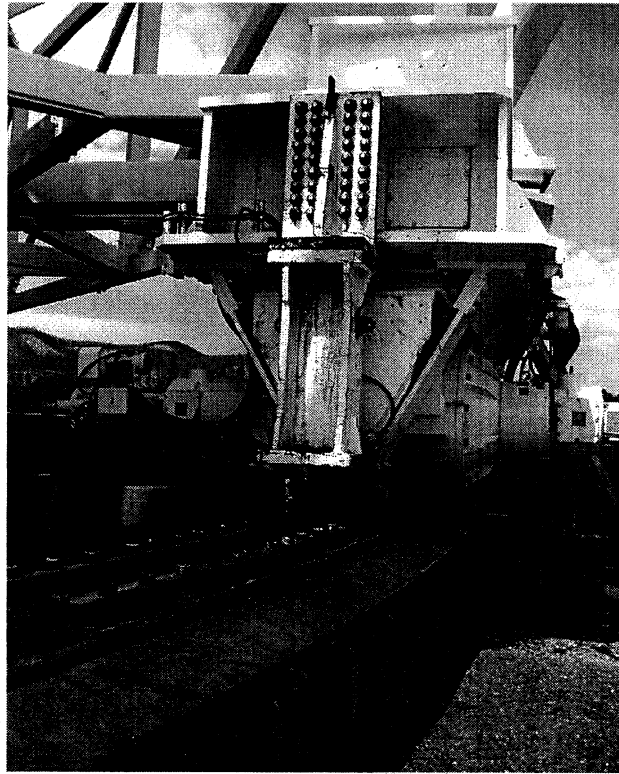


Figure 2.8: End view of wiffle beam. Note lifting fixture and flex plate suspension.

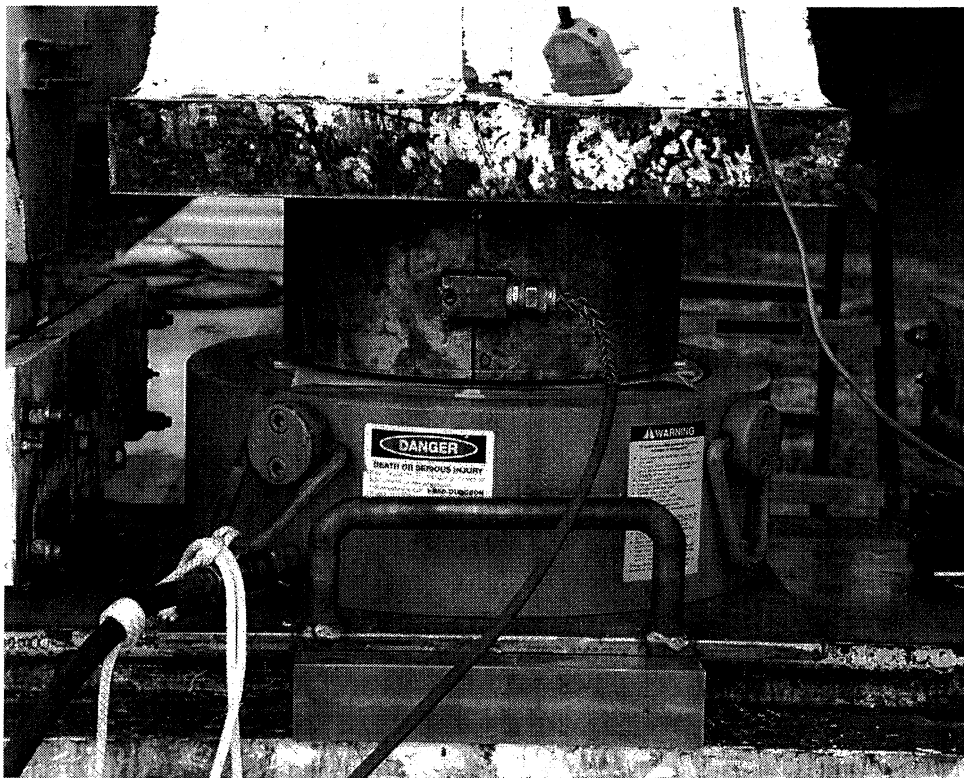


Figure 2.9: Initial load cell configuration.

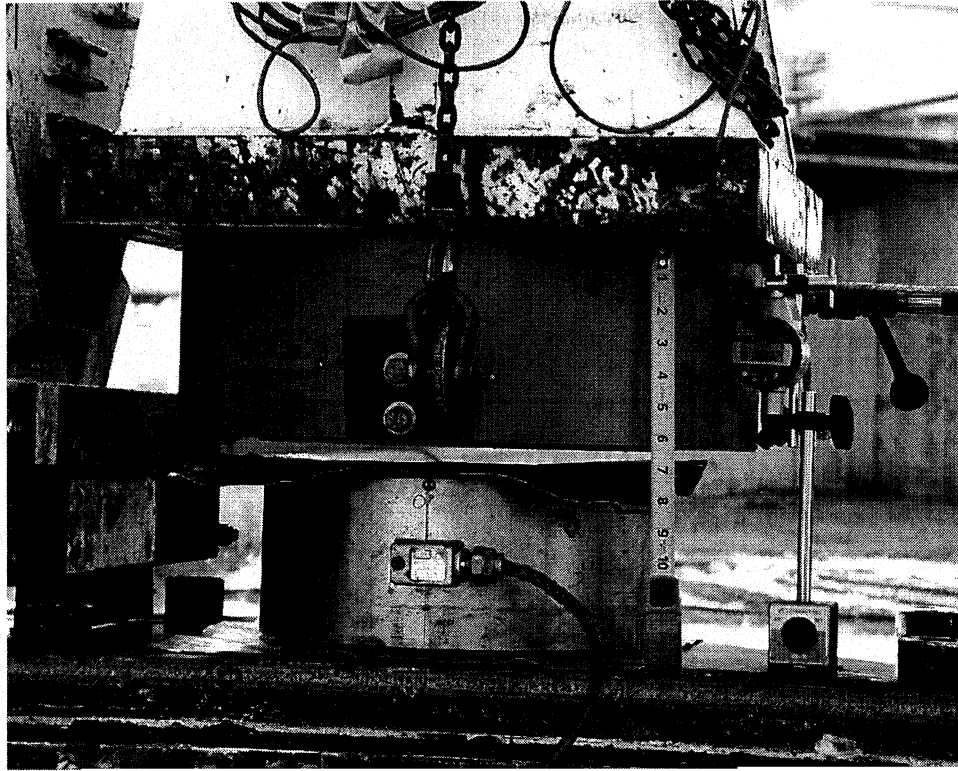


Figure 2.10: Revised load cell configuration.

70 arc seconds. One set of data was taken at that stage of the lift. The wiffle beam was then lifted an additional  $\approx 0.030$ ", which resulted in a rotation of the corner weldment of around 100 arc seconds, to get the second set of data in order to determine the spring constant. It was then lowered back by  $\approx 0.030$ " and a repeat set of data was taken with the wheels just cleared.

The final procedure was:

- configure as track/lead/load cell/lead/jack/fixture
- spray lead sheets with WD-40
- pre-lift until wheels clear the track
- lower jacks to zero hydraulic pressure
- take readings (load cell excitations and outputs, inclinometer, and digital indicators)
- lift until wheels clear track
- take readings
- lift and additional  $\approx 0.030$  inches
- take readings
- lower  $\approx 0.030$  inches (wheels clear)
- take readings
- lower to zero pressure
- free jacks

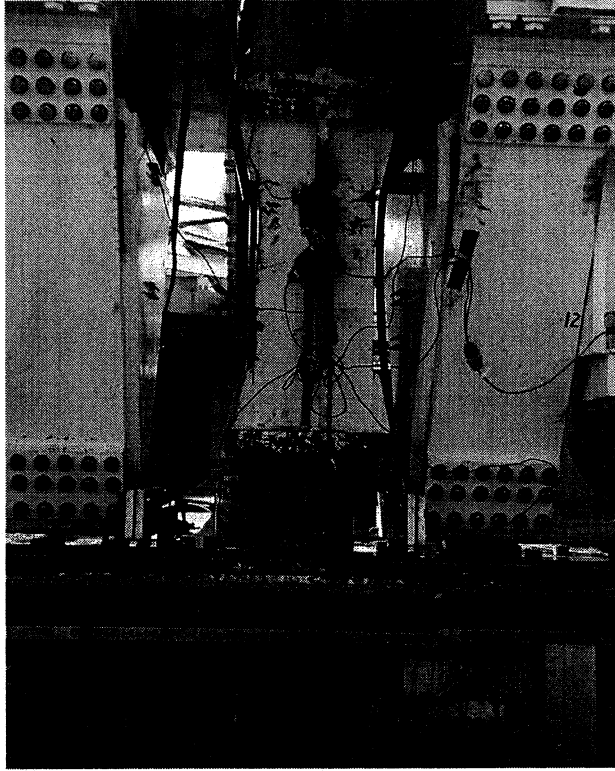


Figure 2.11: Inboard lifting fixture attached to right wiffle beam.

- take readings
- rotate both load cells to the 120 degrees mark and repeat
- rotate both load cells to the 240 degrees mark and repeat
- check repeatability of data—repeat if necessary.

Due to the improved repeatability of the second method, the first three measurements (wheels 1 & 2, 3 & 4, and 5 & 6) were repeated using the second method. Each of these repeat measurements resulted in lower weights (124.0, 51.0, and 105.2 kips). Reproducibility was checked by repeat measurements of, wheels 7 & 8 on 3/24 and 4/8. The two measurements were 1991.1 and 1996.6 kips, for a difference of 5.5 kips, or  $\approx 0.3\%$ .

#### 2.2.4 schedule

As Figure 2.13 shows, the final measurements were completed April 9. With experience, the measurements took 2-3 hours per wheel pair. Movement of the fixtures was labor intensive and required about 4 hours. The fixtures could be left on the telescope, but since the telescope was in use in the evenings, the jacks and load cells could not be prepositioned. Initial set-up in the morning required 1-2 hours. The net result was that by the mechanics working overtime, measurement of one wiffle beam per day was achieved.

#### 2.2.5 included weight

In addition to the GBT structure; all HVAC coolant tanks, diesel tanks, etc., were topped-off at the time of weighing. Receivers included only: L, X, K, Ku, and Q bands; prime focus 1 (800 MHz); and holography.



Figure 2.12: Hydraulic system.

Date	Wheel #s	Truck # or Corner	Jack Position	Lead Condition
3/17/2003	1-2	1	Upright	Dry
3/18/2003	3-4	1	Upright	Dry
3/19/2003	5-6	2	Upright	Dry
3/21/2003	5-6 Repeat	2	Upright	Dry
3/24/2003	7-8	2	Inverted/Upright	Dry/Lubricated
3/25/2003	9-10	3	Inverted	Lubricated
3/26/2003	11-12	3	Inverted	Lubricated
3/27/2003	13-14	4	Inverted	Lubricated
3/28/2003	15-16	4	Inverted	Lubricated
4/2/2003	1-2 Repeat	1	Inverted	Lubricated
4/3/2003	5-6 Repeat 2	2	Inverted	Lubricated
4/8/2003	7-8 Repeat	2	Inverted	Lubricated
4/9/2003	3-4 Repeat	1	Inverted	Lubricated

Figure 2.13: Schedule of Operations.

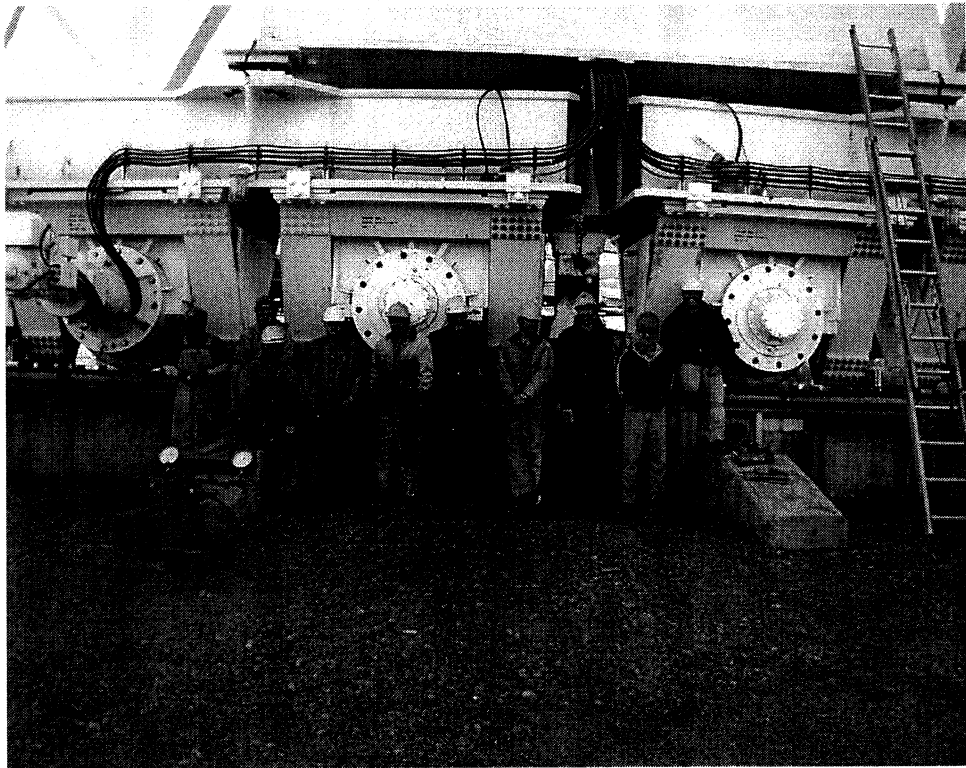


Figure 2.14: Crew (l to r) Shawn Nottingham, Harry Chocklett, Ron Gordon, Bill Radcliff, Preston Meadows, Don Gordon, Troy Fakes, John Shelton (group leader), Jeff Cromer, Edgar Friel, not pictured; Bob Goldizen, Harry Morton.

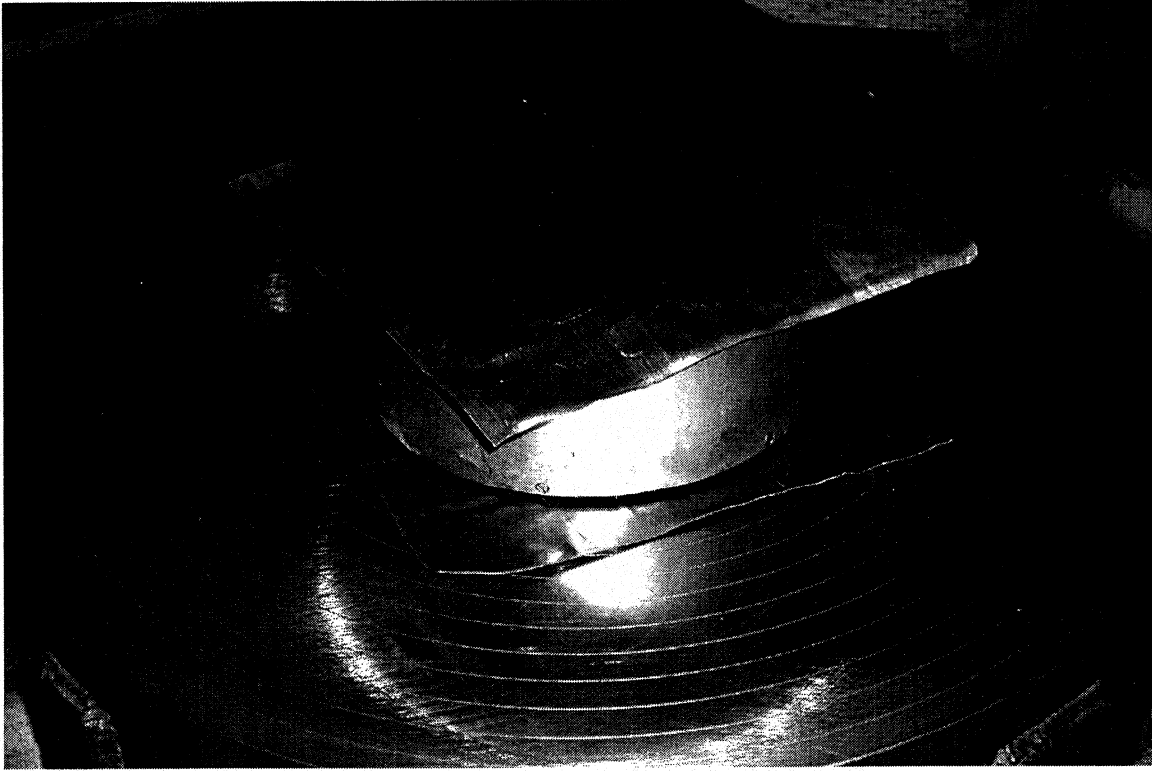


Figure 2.15: Load cell calibration with lead sheets.

### 2.3 Follow-up Load Cell Calibration

Since the load cell end conditions did not match the calibration conditions (sheet lead vs 1/2 inch thick aluminum plates); the load cells, multimeter, and sheets of lead were sent back for a calibration refinement. Dr. Phillips investigated four end conditions on April 18, 2003. First; after checking the contact pressure and determining that it was well below the maximum for the platens, he put a load cell in contact with the bare platens and repeated the calibration. Second; he repeated the March 4 calibration using the 1/2 inch aluminum. Third; he used dry lead sheets, as shown in Figure 2.15. Fourth; he used lubricated lead sheets.

He found very different responses for each condition. This is all well documented in his calibration report in Appendix J, but most notable is that the aluminum plates repeated the initial calibration, but the bare platens had a significantly lower output than the aluminum plates! Moreover, the lead sheets were non-linear and the initial loading showed significant hysteresis! The slopes of the curves for all four end conditions had a range of  $\approx 13\%$ . This clearly had to be addressed.

After looking at the first four experiments, and thinking about the conditions under which the field measurements were made, i.e., all loads were in the 1200 kip range with lead end conditions, we decided to use the slope of the 0-2000 kip curve, in the neighborhood of 1200 kips and to force the curve to pass through a point loaded to only 1200 kips the second and third time, i.e., load it to 1200, 1210, and back to 1200 kips, three times and use the last four outputs at 1200 kips. This more closely duplicated the actual measurement conditions, i.e., we never loaded to 2000 kips in the field.

Using this method, we estimated the 1200 kip outputs to be 0.8280 mV/V for serial #1976; and 0.8503 mV/V for serial #2081. The slopes in the neighborhood of 1200 kips were 0.000 620 7 mV/V/kip for serial #1976; and 0.000 618 5 mV/V/kip for serial #2081, or

$$V_{\text{out}} = (0.000\ 620\ 7 * F + 0.083\ 1)V_{\text{in}} \quad (2.1)$$

for serial #1976; and

$$V_{\text{out}} = (0.000\ 618\ 5 * F + 0.108\ 1)V_{\text{in}} \quad (2.2)$$

for serial #2081;  
where  $V_{\text{out}}$  is in mV,  $V_{\text{in}}$  is in V, and  $F$  is in kips.

# Chapter 3

## Results

### 3.1 Treatment of Data

Using the April 18 calibration equations, each Voltage measurement was converted to kips. The sum of both load cells and the corresponding corner weldment angles were paired for all measurements of a particular wiffle beam, e.g., (2226.0 kips, 80 arc seconds), (2224 kips, 90 arc seconds), etc. In order to calculate the spring constant,

$$\Delta F/\Delta\alpha \tag{3.1}$$

was calculated for both the ascending (typically  $\alpha \approx 60 \rightarrow 90$  seconds) and descending (typically  $\alpha \approx 90 \rightarrow 60$  seconds). The histogram of the ascending  $\Delta F/\Delta\alpha$ , shown in Figure 3.1, shows a good distribution with an average of 0.6719 kips/second and a standard deviation of 0.3049 kips/second. The histogram for the descending  $\Delta F/\Delta\alpha$ , shown in Figure 3.2 also shows a good distribution—but a lower average of 0.4563 kips/second with tighter standard distribution of 0.1924 kips/second.

This difference in the ascending and descending distributions is probably meaningful and most likely related to the friction in the spherical bearings. In the absence of a clear picture, we simply used the average of 0.5641 kips/second as the typical spring constant for all corner weldments. Using this correction, the (F,  $\alpha$ ) pairs were converted to a corrected force for zero  $\alpha$  (wheels on track) by

$$F = F(\alpha) - 0.5641\alpha. \tag{3.2}$$

The angle corrected force was then corrected for the additional weight of the jacks (540 lbs each), and fixtures/bolts (3550 lbs each) for a total of 8.18 kips for each wiffle beam.

Parallel calculations were made using the hydraulic pressure readings and an assumed piston area of 201.2 in<sup>2</sup>, as shown in the histograms in Figures 3.3 and 3.4. The average  $\Delta F/\Delta\alpha$  for the ascending distribution is 0.6132 kips/second with a standard deviation of 0.2889 kips/second. The average for the descending distribution is 1.3342 kips/second with a standard deviation of .5434 kips/second. This yields an average  $\Delta F/\Delta\alpha$  of 0.9793 kips/second—or about 70% larger than the load cell measured spring constant.

Note that the ascending hydraulic spring constant is in much closer agreement with the load cell spring constant. This would suggest that there is significant hysteresis in the jack pressure for a small ( $\approx 0.03^\circ$ ) reversal of direction, which could be a result of additional friction when the seals reverse direction. As a test on the frictional force on the jacks, we looked at the load cell forces for cases where the hydraulic pressure was released, but the jacks were not forced down mechanically, e.g., after a prelift. The histograms in figures 3.5 and 3.6 show the distribution for the load cells. Note that the residual forces/standard deviations for load cells 1976 and 2081 were 11.6/1.1 and 26.3/2.5 kips. Recall that the calibration curves were optimized for the 1200 kip neighborhood, so the large residuals are an artifact of the calibration curves. Figures 3.7 and 3.8 shows similar histograms for actual zero load measurements which show forces/standard deviations for load cells 1976 and 2081 as 11.3/1.3 and 24.3/1.1 kips. The differences between the residual jack force and true zeros are of the order of the standard deviations for both cells, so about all we can say is that the friction of the jacks was less than a few kips and the repeatability of the load cell zeros are around 1 kip.

**Histogram of Delta Force / Delta Angle from Load Cell Force**  
 Data from wheels clear to plus .030 Average: .6719 Standard Deviation: .3049  
 File: Zeropoints-temp.xls Disk: C17

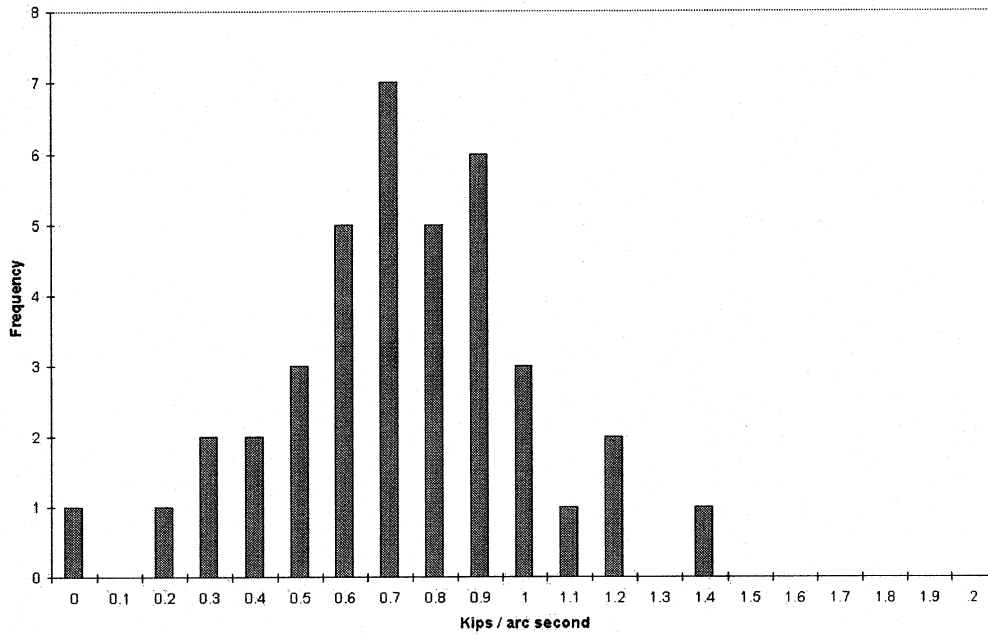


Figure 3.1: Histogram of ascending  $\Delta F/\Delta\alpha$  for load cells.

**Histogram of Delta Force / Delta Angle from Load Cell Force**  
 Data from plus .030 to wheels clear Average: .4563 Standard Deviation: .1924  
 File: Zeropoints-temp.xls Disk: C17

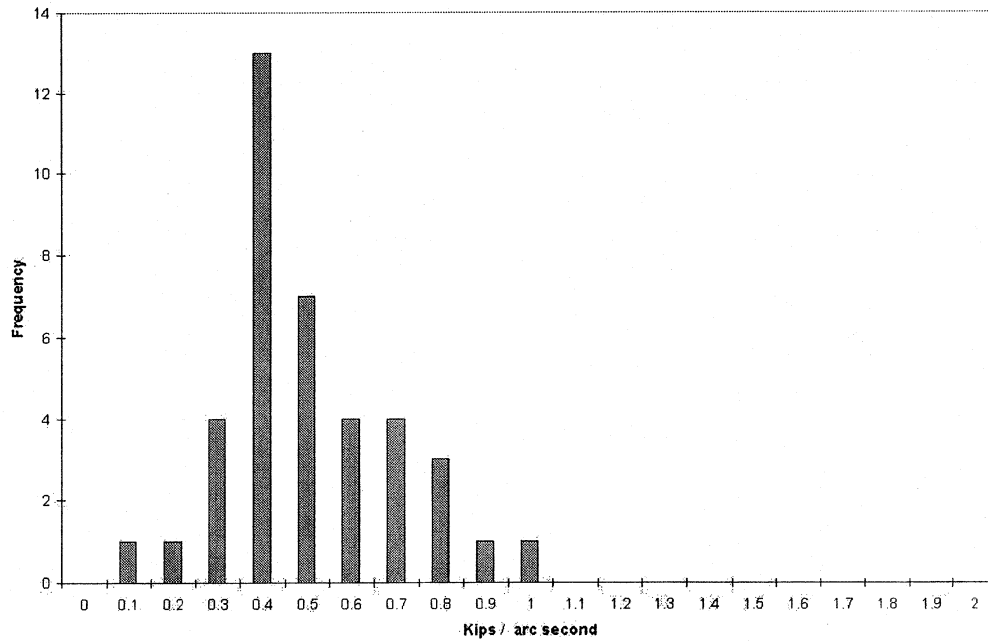


Figure 3.2: Histogram of descending  $\Delta F/\Delta\alpha$  for load cells.

Histogram of Delta Force / Delta Angle from PSI  
 Data from wheels clear to plus .838 Average: .6132 Standard Deviation: .2689  
 File: Zeropoints-temp.xls Disk: C17

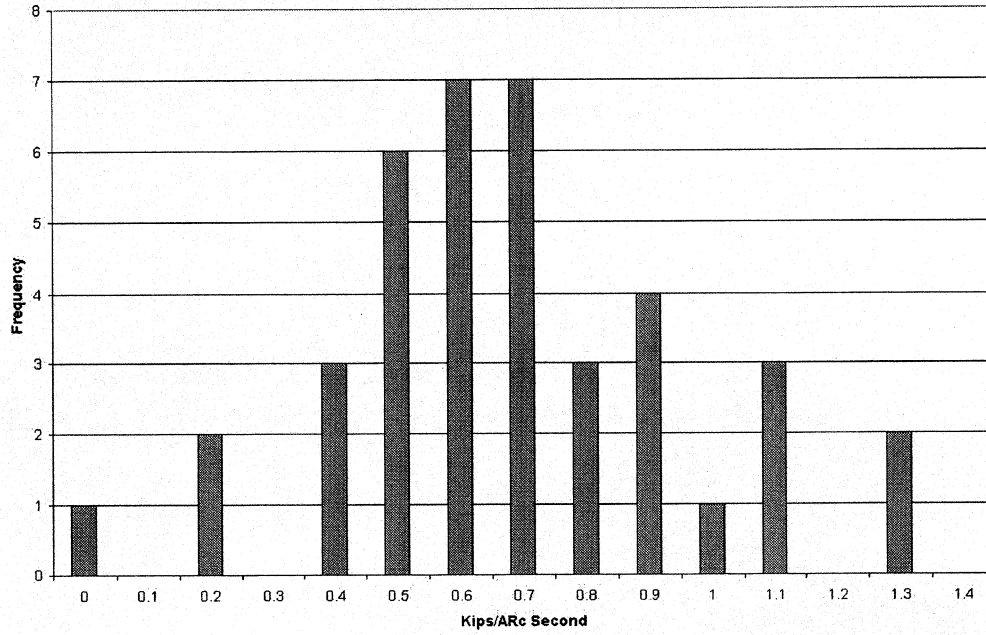


Figure 3.3: Histogram of ascending  $\Delta F/\Delta\alpha$  for hydraulic pressure.

Histogram of Delta Force / Delta Angle from PSI  
 Data from plus .838 to wheels clear Average: 1.3342 Standard Deviation: .5434  
 File: Zeropoints-temp.xls Disk: C17

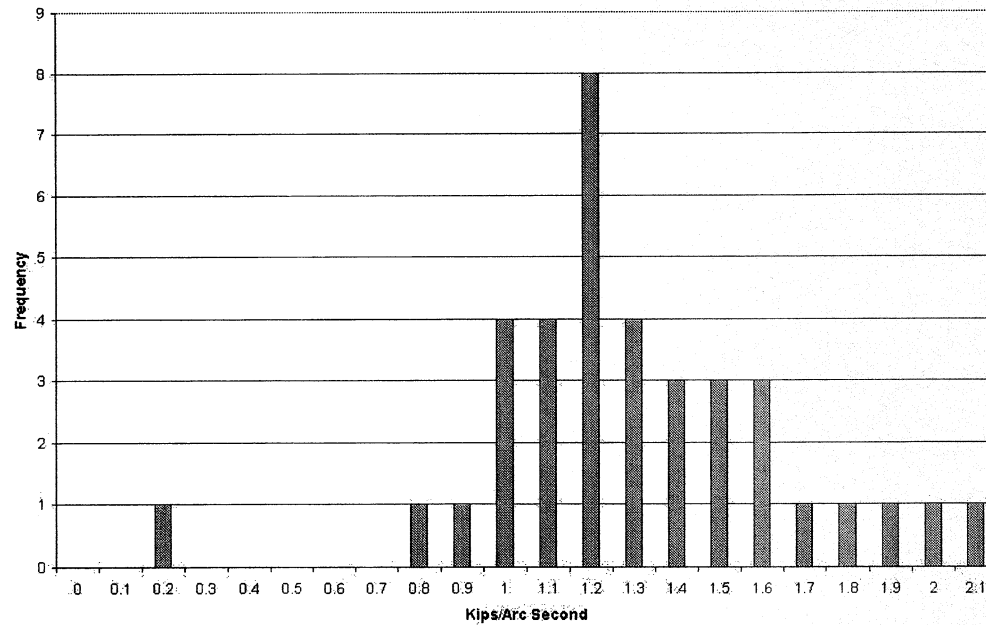


Figure 3.4: Histogram of descending  $\Delta F/\Delta\alpha$  for hydraulic pressure.

**Histogram of Force on Load Cell 1976**  
 Jacks are not retracted File: Zeropoints-temp.xls Disk: C17  
 Average: 15.0 Standard Deviation: 1.107

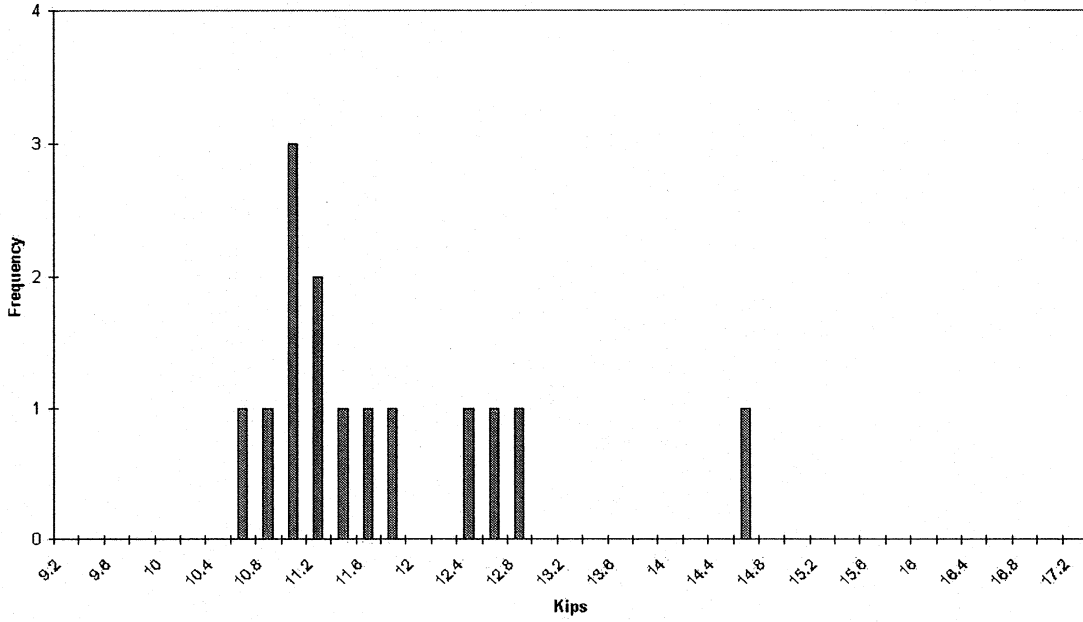


Figure 3.5: Histograms of residual load cell force on cell 1976—including jack friction.

**Histogram of Force on Load Cell 2081**  
 Jacks are not retracted File: Zeropoints-temp.xls Disk: C17  
 Average: 29.5 Standard Deviation: 2.519

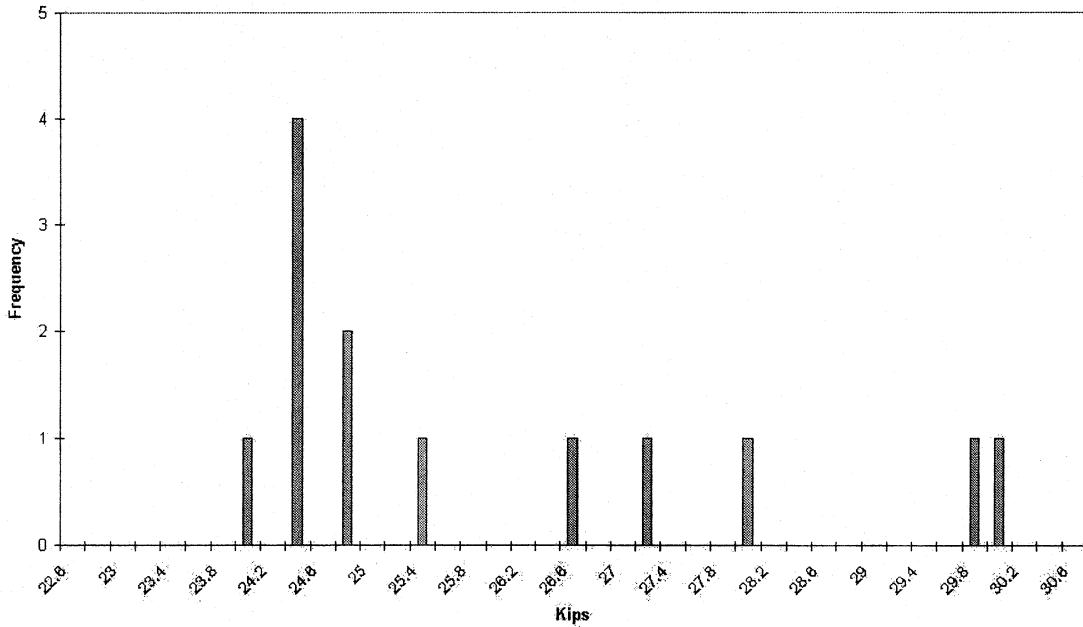


Figure 3.6: Histograms of residual load cell force on cell 2081—including jack friction.

**Histogram of Force on Load Cell 1976**  
 Jacks are retracted File: Zeropoints-temp.xls Diek: C17  
 Average: 11.3 Standard Deviation: 1.279

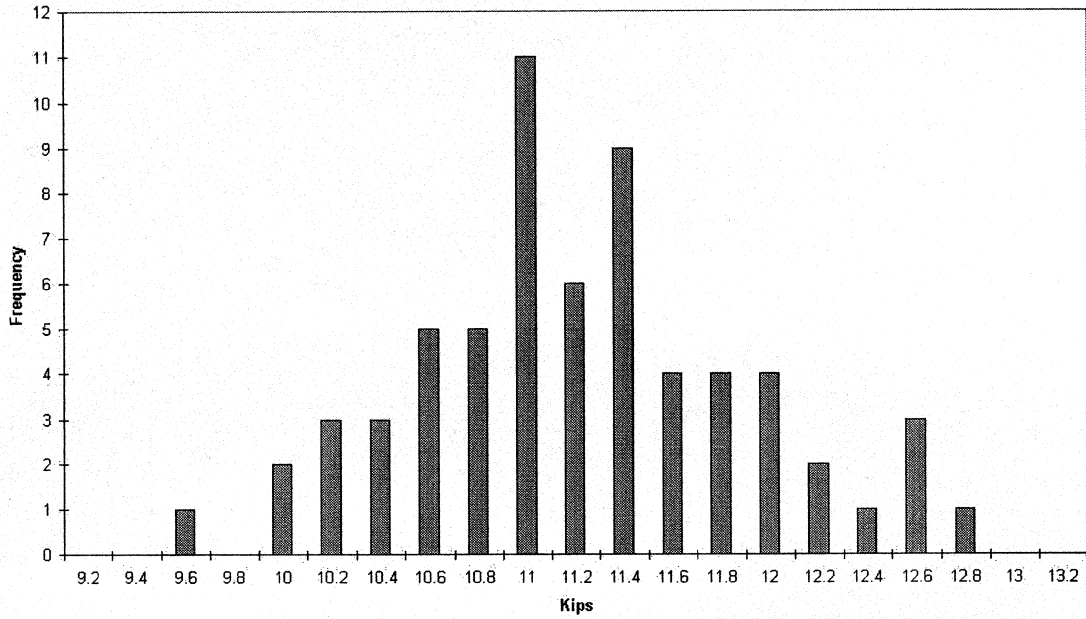


Figure 3.7: Histograms of zero force on cell 1976.

**Histogram of Force on Load Cell 2081**  
 Jacks are retracted File: Zeropoints-temp.xls Diek: C17  
 Average: 24.3 Standard Deviation: 1.095

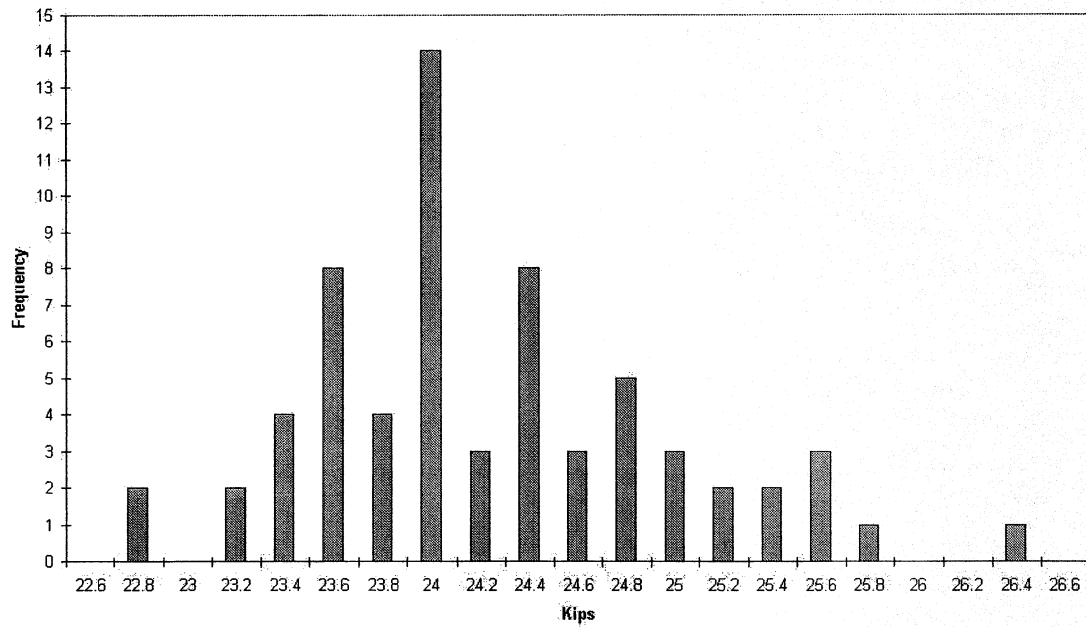


Figure 3.8: Histograms of zero force on cell 2081.

Summary of GBT Rolling Weight				Date: April 22, 2003	
*Based on second load cell calibration					
Corner #	Wheels	Force (kips)	Standard Deviation (kips)	Range (kips)	Total Forces (kips)
1	1+2	2189.612	10.845	31.907	
1	3+4	2151.062	7.734	22.082	4340.675
2	5+6	2050.505	4.789	15.487	
2	7+8	1999.637	6.484	19.337	4050.142
3	9+10	2035.494	6.880	21.684	
3	11+12	2041.290	8.297	26.754	4076.784
4	13+14	2060.010	14.486	36.887	
4	15+16	2199.348	10.028	27.938	4259.358
Overall Total					16726.958
Standard Deviation			26.764		
*Based on PSI readings					
Corner #	Wheels	Force (kips)	Standard Deviation (kips)	Range (kips)	Total Forces (kips)
1	1+2	2206.071	11.758	34.570	
1	3+4	2120.830	10.340	25.160	4326.902
2	5+6	2060.004	8.620	23.147	
2	7+8	2021.089	8.990	24.154	4081.093
3	9+10	2009.787	9.264	25.650	
3	11+12	2003.788	6.960	17.952	4013.575
4	13+14	2055.574	10.263	31.010	
4	15+16	2182.499	12.566	39.766	4238.073
Overall Total					16659.642
Standard Deviation			29.725		

Figure 3.9: Summary of GBT rolling weight.

## 3.2 Calculated Weights

Using the second method data; the angle and jack/fixture load corrections were made. The average, standard deviation, and range were calculated for each wheel pair, using both the load cell and hydraulic pressure, as shown in Figure 3.9. Note that the statistics are for a minimum of 9 measurements (clear, clear plus  $\approx 0.030''$ , clear-for three rotations of the load cells).

For the load cells, the total weight is 16 727 kips with a standard deviation of 26.7 kips. The hydraulic pressure calculation resulted in a remarkably close (0.4 %) agreement of 16 660 kips with a standard deviation of 29.7 kips—even though a much larger spring constant was used and individual wheel pairs differed by as much as 1.8%.

## 3.3 Estimation of Uncertainty

There are three principal contributions to the combined standard uncertainty,  $u_c$ , of the total GBT weight.

1. load cell calibrations
2. estimation of the spring constant
3. repeatability of the measurements

Using the procedures outlined in NIST Technical Note 1297, Guideline for Evaluating and Expressing the Uncertainty of NIST Measurement Results[12], which is in compliance with ISO 9000 standards, the standard uncertainty of the individual load cell calibrations,  $u_1$ , were estimated to be 2 kips. Since the two cells were combined for all measurements, we can take the root-sum-of-squares, RSS, for the pair as 3 kips.

The estimation of the uncertainty due to the spring constant is a little less obvious. We clearly see a difference in the  $\Delta F/\Delta \alpha$  for the ascending (0.6719 kips/second) and descending (0.4563 kips/second)

histograms. If we assume the true value is somewhere between the two cases and assume a rectangular distribution, as in section 4.6 of TN 1297, then the standard uncertainty of the spring constant would be  $\Delta/2\sqrt{3} = 0.062$  kips/second, or  $\approx 11\%$ . Since the same spring constant was applied to all 8 weights, and the average  $\alpha$  was 80 seconds, the standard uncertainty due to the spring constant,  $u_2$  would be

$$u_2 = 0.062 * 80 * 8, \tag{3.3}$$

or 39.7 kips.

From Table 3.9, the standard deviation of the weights,  $u_3$ , was 26.7 kips. The combined standard uncertainty (level of confidence of  $\approx 68\%$ ),  $u_c$ , is the RSS of the standard uncertainties i.e.,

$$u_c = (3^2 + 39.7^2 + 26.7^2)^{1/2}, \tag{3.4}$$

or  $u_c \approx 48$  kips, for a relative combined standard uncertainty of 0.3%.

## Chapter 4

# Auxiliary Measurements

While lifting the telescope, auxiliary measurements were also made for each lift. Indicators were used to measure the jack strokes. Indicators were placed between the wheel housing and wiffle beams to measure the vertical movement due to the relaxation of the flex plate suspension system. An indicator was used to measure the circumferential motion of the idler wheels. The manufacturer built-in a “pointer” and reference mark, used to measure twist of the suspension system, on each assembled wheel, i.e., with the wheel floating freely, the pointer was centered on a reference mark. All pointer readings were recorded before lifting, with the wheels clear, and after lowering back to the track.

Additional indicator readings were taken on a pair of flex plates to measure the actual length relaxation, and across the wiffle beam, in search of an explanation for some unexpected results in the magnitude of the wheel housing to wiffle beam data—which remains unexplained.

### 4.1 Jack Stroke Measurements

The wheels and jack locations were identified with respect to the line of symmetry through the center of the corner of the telescope as outboard and inboard, e.g., the two wheels on the outside of the four wheel arrangement were identified as the outboard wheels, and the two nearest the center were identified as the inboard wheels. Both jack strokes were measured as shown in Figure 2.10. As shown in Figure 4.1, the jack strokes were repeatable and about 0.35 inches of stroke was required for the wheels to clear the track. Note that this is  $\gg$  0.125 maximum lift at the top of the wiffle beam. After the load had all been transferred from the wheels to the jacks, the movement became linear, i.e., an additional 0.030 inch produced a linear twist of the corner weldment. Recall that the jack fixtures are on the end of the wiffle beam. Shifting the vertical load from the wheels to the ends of the wiffle beams resulted in a visibly noticeable bending of the wiffle beam, and thus the large jack strokes.

### 4.2 Wheel Housing-to-Wiffle Beam

The pairs of flex plates on each wheel suspension system were identified as distal and proximal, with respect to the corner center, e.g., the flex plates on wheel 1, closest to wheel 2, are the outboard proximal flex plates.

Figure 4.2 shows how the digital indicators were positioned between the wheel housing and the wiffle beam in order to measure the motion due to relaxation of all four pairs of flex plates on a wiffle beam. There was a very interesting discovery in the data, as shown in Figure 4.3. Note that the motions were very repeatable—but in all cases; the flex plates next to the jacks (outboard distal and inboard proximal) measured significantly larger deflections than the flex plates near the center of the wiffle beam (outboard proximal and inboard distal).

On the repeat measurements of wheels 1 & 2, 4 indicators were set up on wheel 1 near each flex plate. These measurements, shown in Figures 4.5 and 4.6, on each side agreed with the center measurements, i.e., symmetrically larger motions, on each side, for the pair of flex plates next to the jack.

Similar measurements were made on the inboard proximal end of the idler wiffle beam, as shown in Figure 4.4. Note that the relaxation was 0.001–0.002 inches, i.e., the load on the idler wiffle beam was

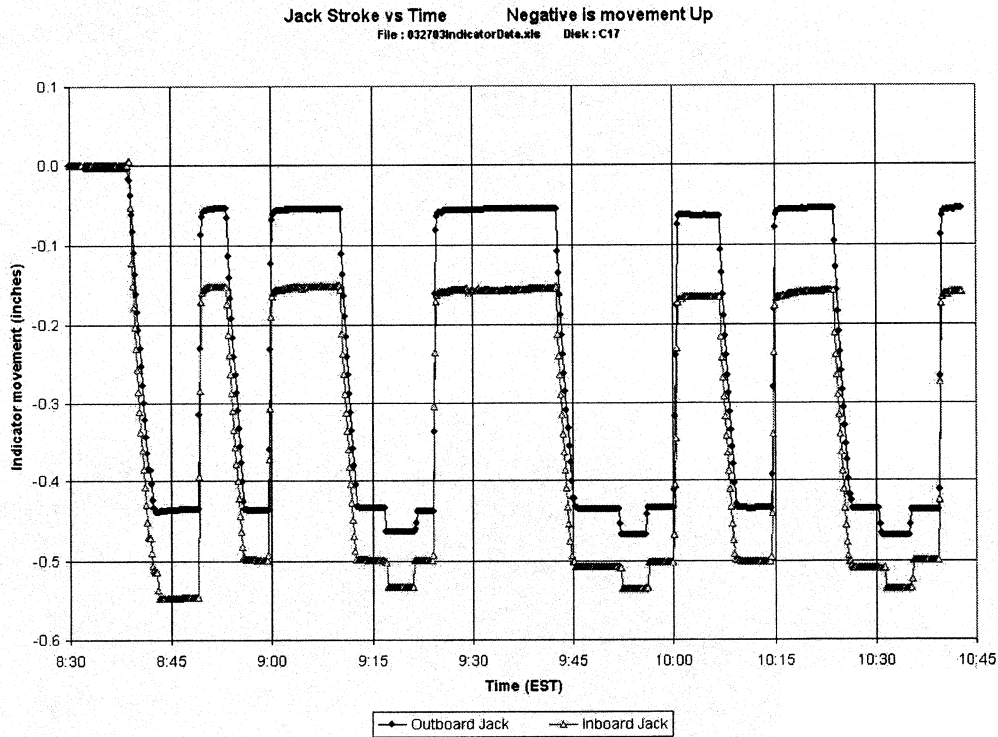


Figure 4.1: Typical jack stroke measurement data

slightly reduced while lifting the companion wiffle beam.

#### 4.2.1 wheel 13

Wheel 13 ran over an object on the track in March 2002. The details are not clear, but the resulting travel of the wheel suspension was such that telltale marks were left on the wiffle beam housing. Analysis of the housing to wiffle beam plots of wheel pair 13/14 on 3/27 (included in the Appendices) shows that the deflections of wheel 13 are nominal for the proximal flex plates, at  $\approx 0.050$  inches; but larger than nominal for the distal flex plates, at  $\approx 0.090$  inches vs a consistent nominal of  $\approx 0.070$  for all other wheels. Subsequent to the discovery of the 2002 incident, all flex plates were measured for bow, and wheel 13 flex plates were found to be slightly bent (see report A0289 for details), which probably explains the asymmetry.

### 4.3 Horizontal Deflection of Wiffle Beam

Following up on the asymmetric vertical motions, one theory was that in addition to the jacking fixtures introducing a camber along the circumferential direction of the wiffle beam, the wiffle beam was also deformed by lifting in the center, and thus actually shortening the horizontal distance between the top of the flex plates. A rod was used to span across the horizontal beam, of the 3/27 measurement of wheels 13/14, as shown in Figure 4.7 (with the lifting fixture removed for clarity). One end was fixed to the housing, and the other end pushed against the digital indicator, which was also fixed to the housing.

As the plots in Figure 4.8 show, there was in fact significantly more compression of the horizontal beam next to the jack, e.g.,  $\approx 0.022$  vs  $\approx 0.009$  inches. In retrospect, it is clear from the design of the wiffle beam, that the load was intended to be carried by the side plates, i.e., the flex plates and spherical bearings are all centered on the side plates. The lifting fixtures in the center of the wiffle beam introduce a significant perturbation in the loading.

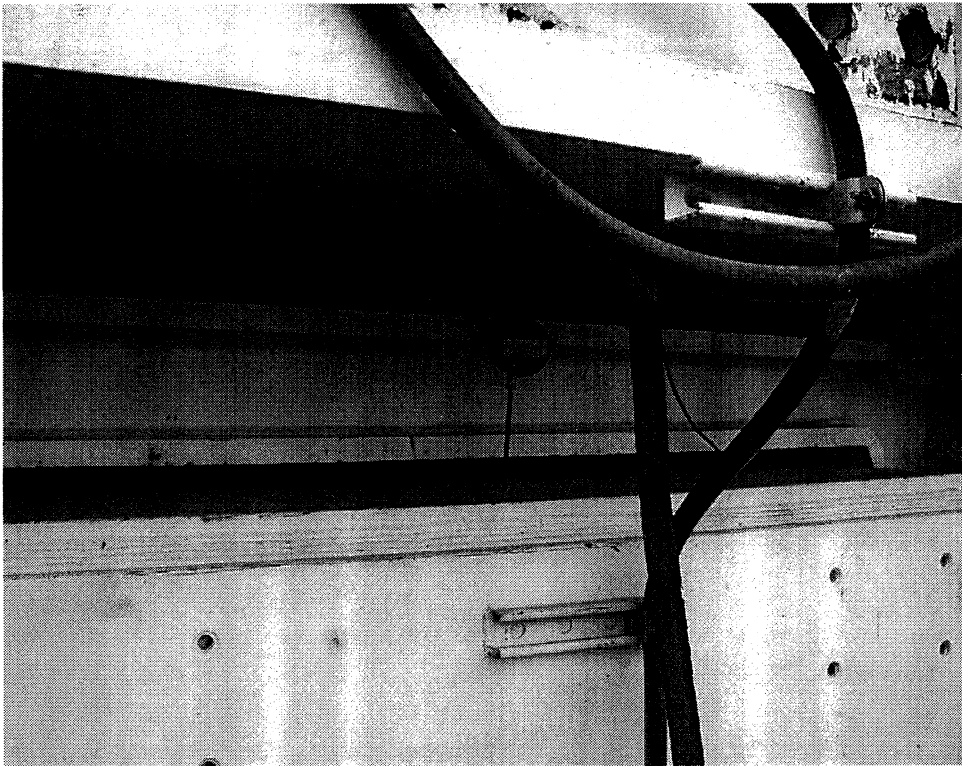


Figure 4.2: .  
Measurement of vertical motion between wheel housing and wiffle beam—lifting fixture removed for clarity.

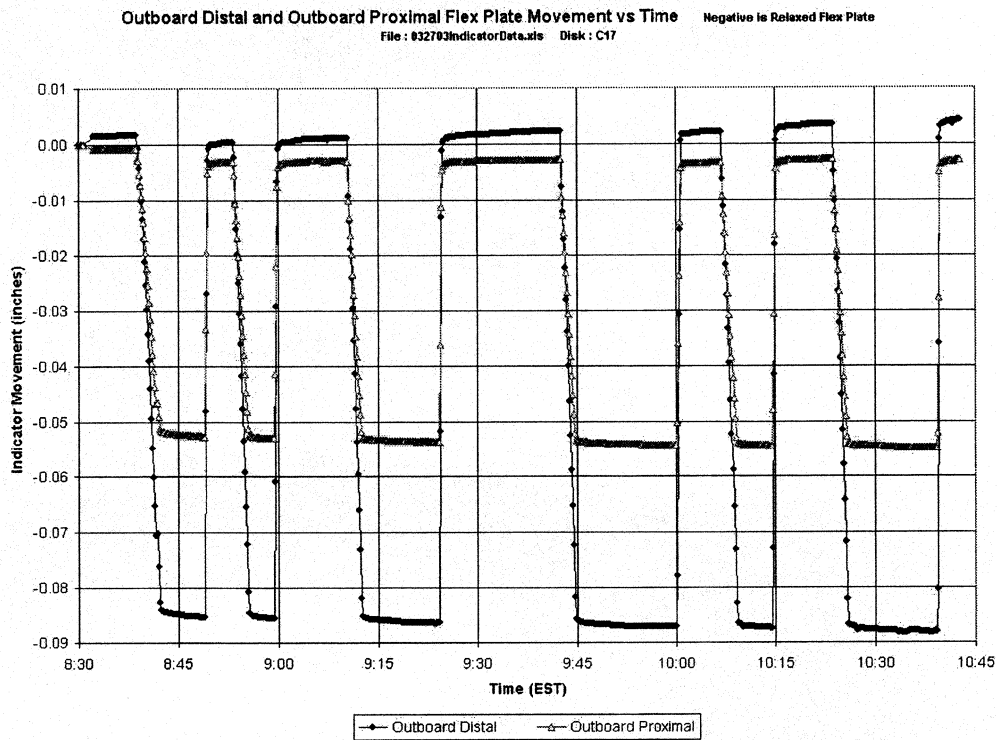


Figure 4.3: Vertical movement between wheel housing and wiffle beam-jacking beam.

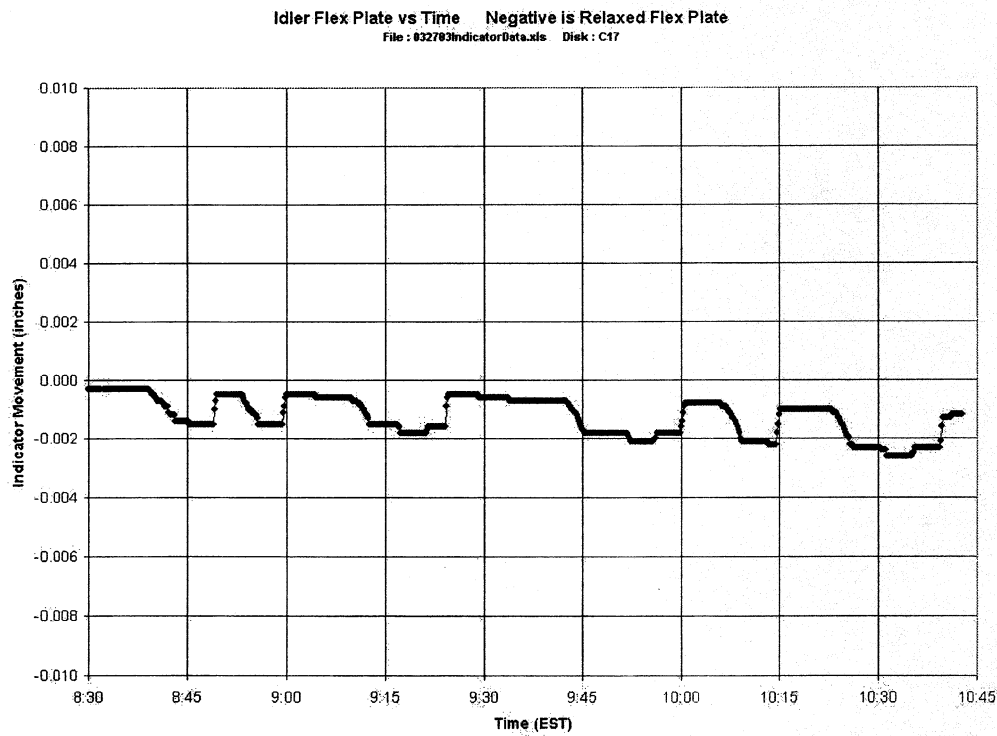


Figure 4.4: Vertical movement between wheel housing and wiffle beam-idler beam.

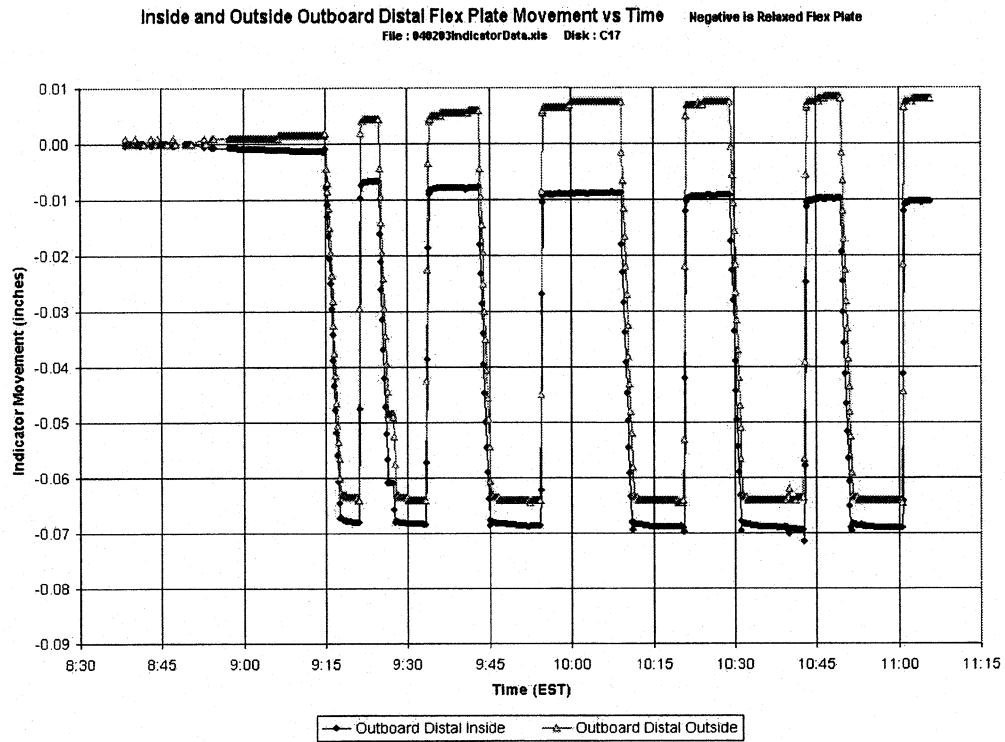


Figure 4.5: Measurement of vertical motion between wheel housing and wiffle beam at both distal flex plates.

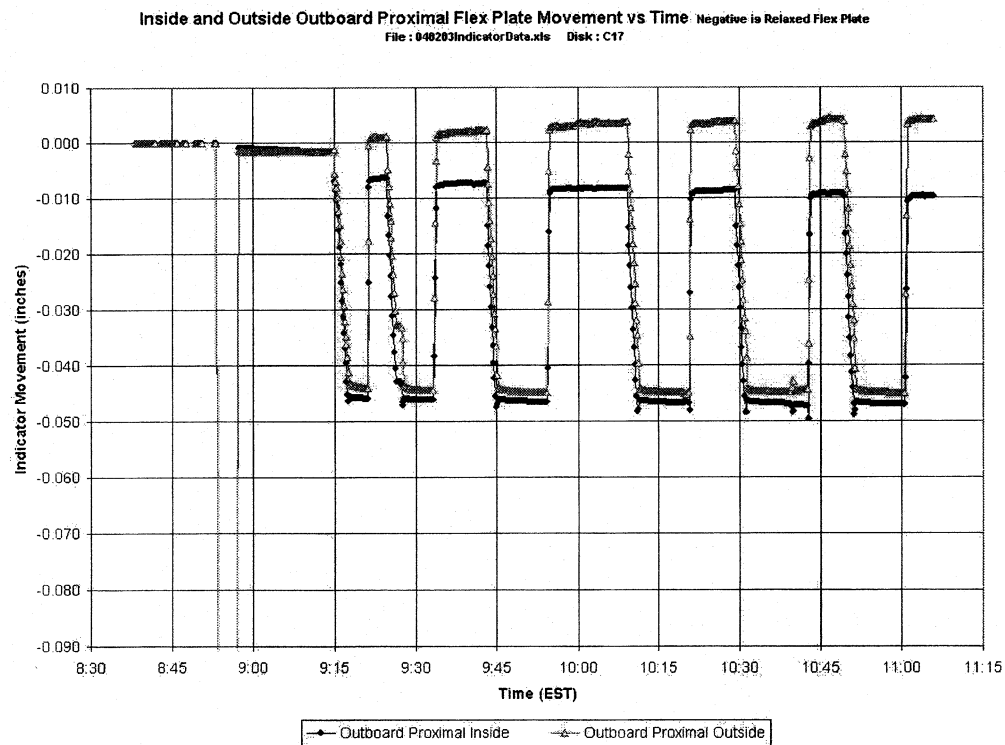


Figure 4.6: Measurement of vertical motion between wheel housing and wiffle beam at both proximal flex plates.

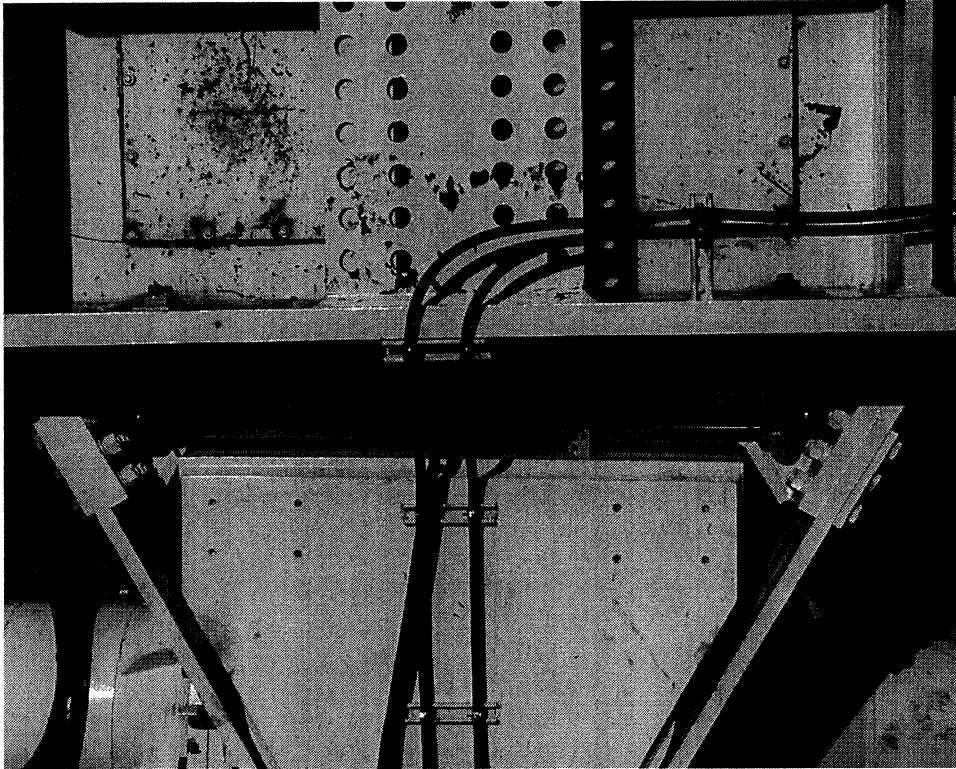


Figure 4.7: Measurement of horizontal deflection of waffle beam.

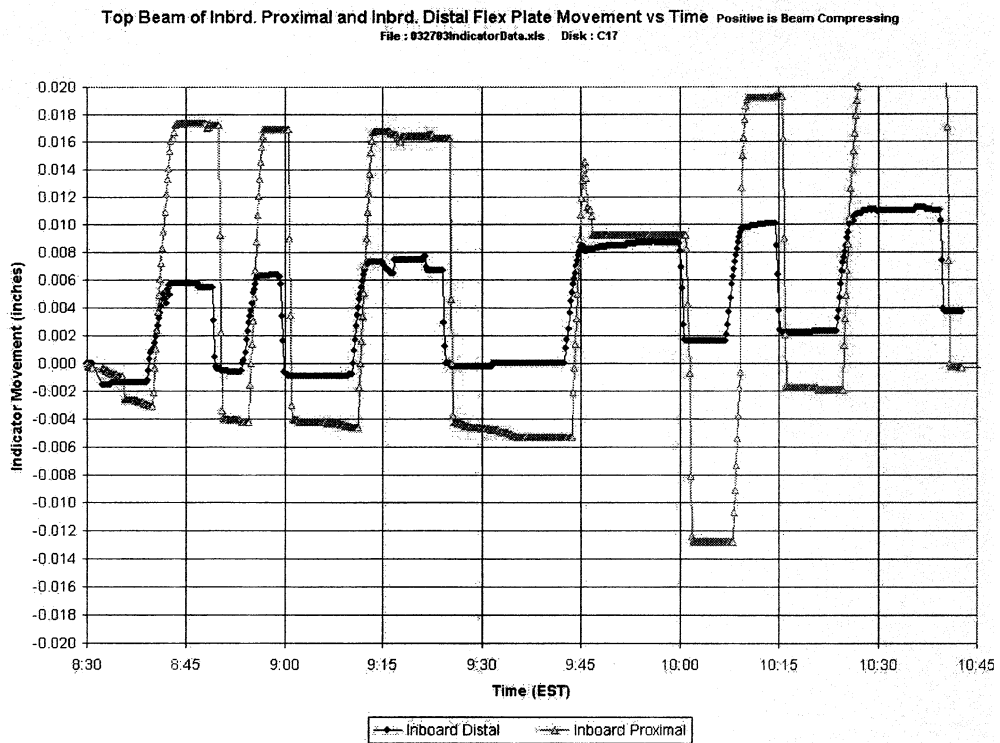


Figure 4.8: Measurement of the compression of the top beams.

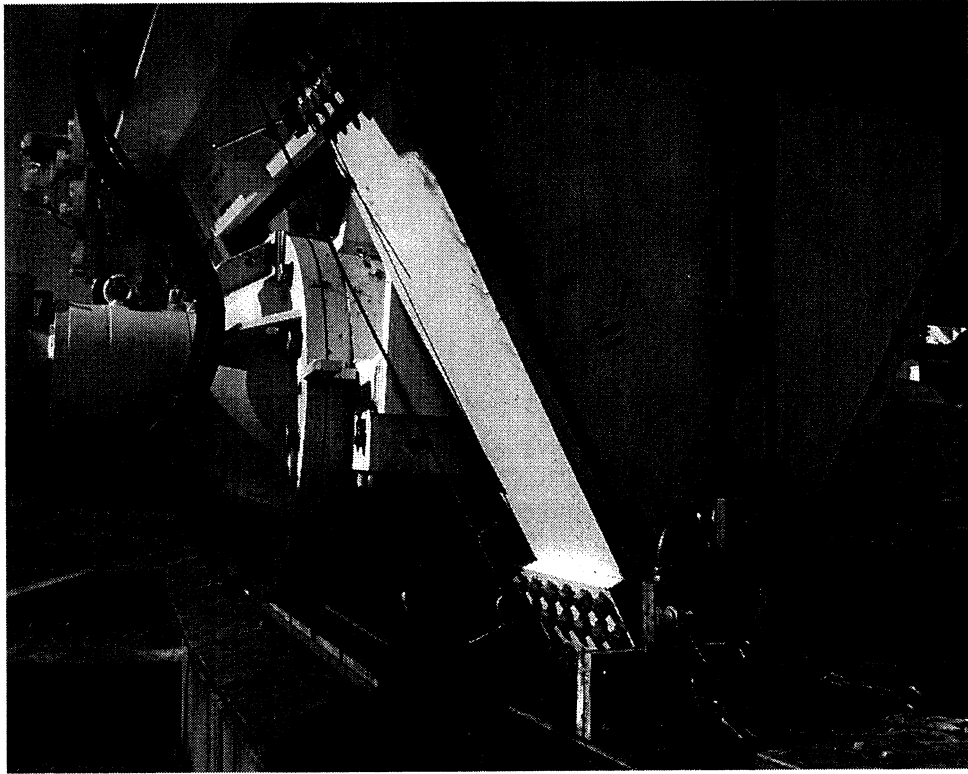


Figure 4.9: Flex plate length measurement.

However, a quick calculation shows that this can not explain the difference in vertical motion between the two pairs of flex plates. The flex plate geometry is approximated by a triangle 73.3 inches across the top (call it  $r$ ), and equal legs of 72.5 on the sides (call them  $l$ ). The change in height of the triangle due to a change in  $r$  can be estimated by

$$h = (l^2 - (r/2)^2)^{1/2} \quad (4.1)$$

$$\partial h / \partial r = -r / 4h \quad (4.2)$$

$$\approx -0.25. \quad (4.3)$$

So, a change in  $r$  of 0.022 inches would only change the height by  $\approx 0.005$  inches, which is much less than measured.

#### 4.4 Flex Plate Length Measurements

Measurements were made of the actual change in length of a pair of flex plates as shown in figures 4.9 and 4.10. The 3/28/03 plots in Figure 4.11 show symmetric length change between full load and no load of  $\approx 0.025$ – $0.028$  inches. Looking at the sensitivity of  $h$  to a change of length,

$$h = (l^2 - (r/2)^2)^{1/2} \quad (4.4)$$

$$\partial h / \partial l = l / h \quad (4.5)$$

$$\approx 1.1, \quad (4.6)$$

so a change in flex plate length  $l$  of 0.03 inches, and the change in  $r$  combined, would not account for the measured change in height of either flex plate—much less the asymmetry.

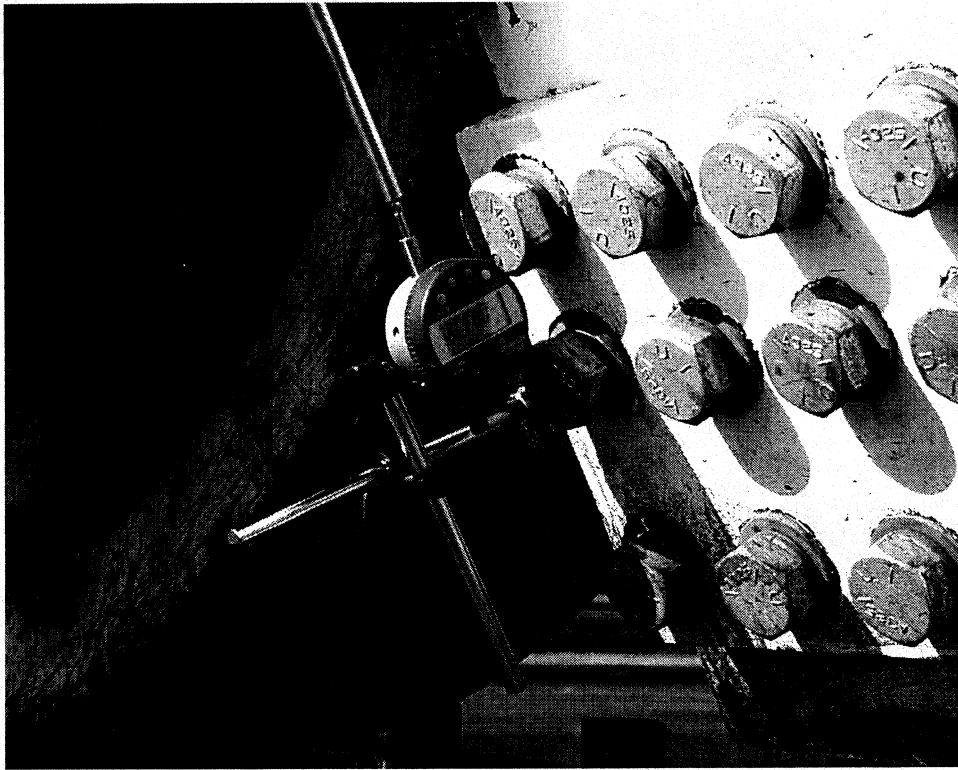


Figure 4.10: Detail of flex plate length measurement.

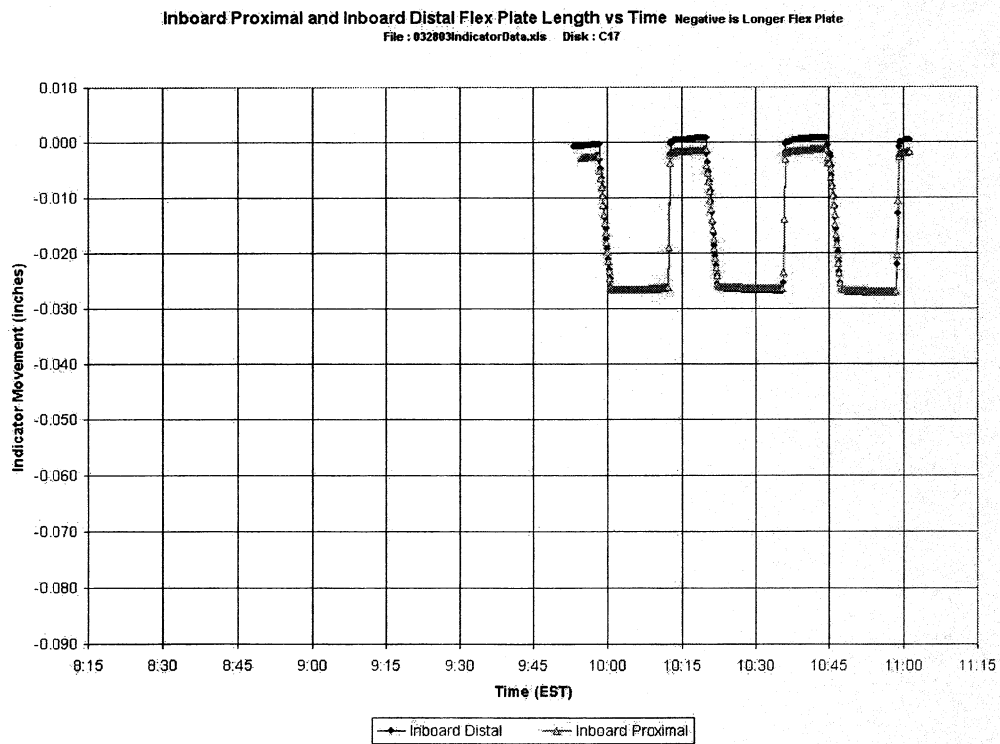


Figure 4.11: Flex plate length data.

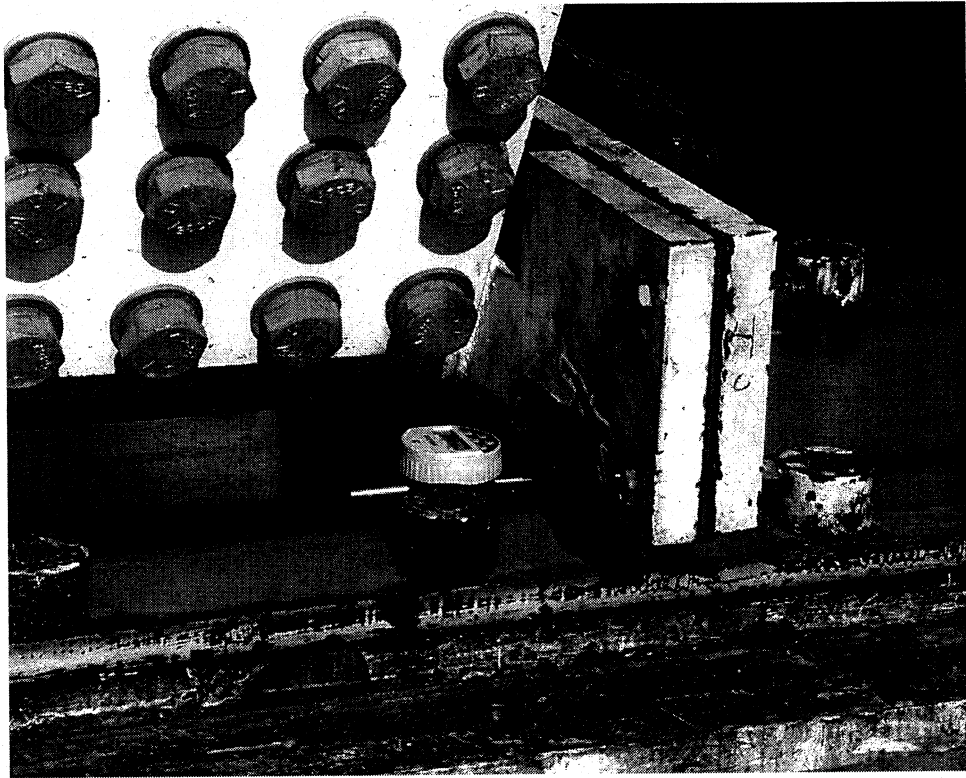


Figure 4.12: Idler circumferential measurement.

## 4.5 Idler Wheel Movement

A digital indicator was used to measure the movement of the idler wheel pair, as shown in Figure 4.12. As shown in Figure 4.13, lifting one waffle beam resulted in the companion pair of wheels rolling toward the jacks by about 0.040 inches. This confirms the need to release the brakes on the companion wheels in order to minimize the lateral force on the load cells. The repeatability of the movement indicates little hysteresis.

## 4.6 Pointer Readings

The mechanical pointers were set to zero for free hanging wheels at the manufacturer. See drawing 121035, sheet 3, view X for details of the pointer design. Near the end of construction, the contractor adjusted the spacers between the wheel housing and waffle beam to insure the nominal loaded wheel pointers remained centered on the zero mark. While the loaded zero mark can be checked routinely, the no load indications had not been checked since 2001.

The pointer readings were recorded in the initial, wheels clear, and back on the track conditions. The table in Figure 4.14 shows that most wheels are no longer centered on zero, and moreover there is a systematic bias in the + direction (tilt toward the pintle).

Idler Rotation vs Time Positive is CW Rotation  
 Error: Indicator positioned on lifting wheel, not idler. Disregard data.  
 File : 032703IndicatorData.xls Disk : C17

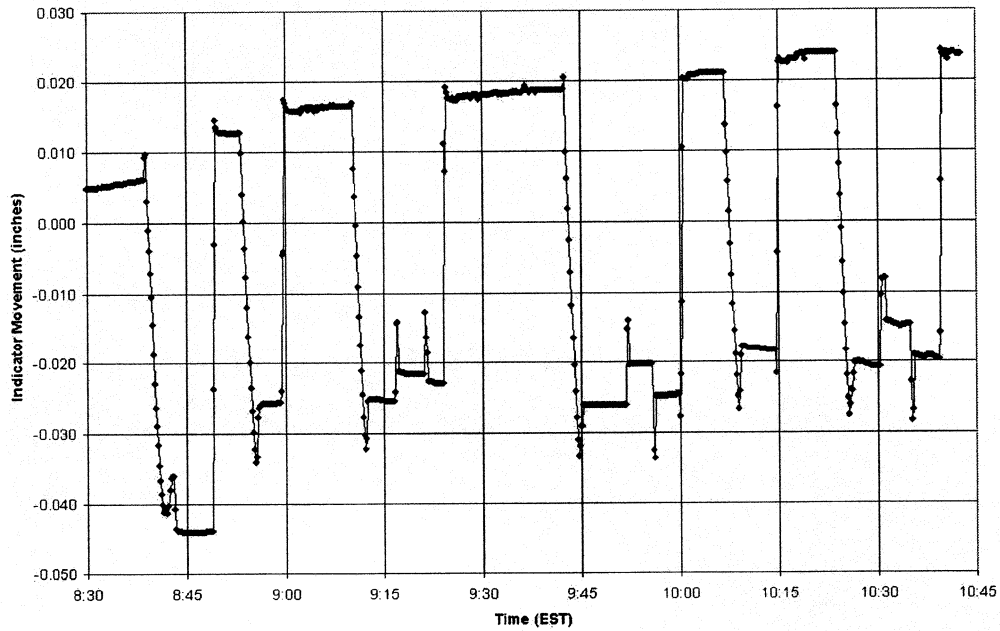


Figure 4.13: Idler wheel movement.

Wheel #	(Truck# -Wheel#)	Avg. In-Air Reading	Avg. On-Track Reading
1	(1-1)	0.06	0.06
2	(1-2)	0.06	0.06
3	(1-3)	No Data	No Data
4	(1-4)	No Data	No Data
5	(2-1)	0.03	0.06
6	(2-2)	0	0.06
7	(2-3)	0.06	0.06
8	(2-4)	0.06	0.06
9	(3-1)	0.06	0.03
10	(3-2)	0.06	0.06
11	(3-3)	0	0.06
12	(3-4)	0.06	0.06
13	(4-1)	0.06	0.04
14	(4-2)	0.05	0.05
15	(4-3)	0.06	0.05
16	(4-4)	0.03	0.02

Figure 4.14: Table of pointer measurements. Positive direction tilts toward pintle.

# Chapter 5

## Summary

### 5.1 Notes on Appendices

These measurements generated a wealth of data—most of which will not be of general interest. Some of it may be of interest at some future date to use as benchmarks to quantify changes, or as checks on finite element model predictions. All of this data, as well as a number of photographs, are retained in the Appendices, and on the CD ROM. A Power Point presentation is also included on the CD.

### 5.2 Acknowledgments

Thanks to a number of people that responded with valuable advice on this project, including: Rick L. Seifarh, NIST Force Calibration Lab; Joel Treshansky, Marshal Space Flight Center Calibration Lab; Guy Petrillo, Richard Dudgeon, Inc.; and Dr. James W. Phillips, University of Illinois at Urbana-Champaign.

# Bibliography

- [1] Engineering Data, 100 Meter Telescope, drawing 121003, 5/9/91.
- [2] Module 8R weight-experimental results, A0117, 7/1/98.
- [3] Weight & Balance Analysis-Elevation Rotating Structure, Tech Memo 38, revision 3, 9/29/99.
- [4] Azimuth Wheel Bearing Replacement Procedure 121967, 9/19/00.
- [5] Installation, Jacking, Wiffle Beam and Corner Weldment, drawing 121557 rev AS, 8/15/00.
- [6] Wiffle Beam, drawing 121033 rev H.
- [7] Jacking Procedure-Azimuth Wheel Assembly & Corner Weldment.
- [8] NIST Calibration Services Users Guide, 1998
- [9] Report on Management Experiences From the Green Bank Telescope Project, Robert J. Wallace, Modern Technologies Corp., 11/15/2002, GBT Archive M0221.
- [10] Options and Methods for Weighing the GBT, David H. Parker, GBT Archive A0322
- [11] Proposed Procedures for Weighing the GBT, David H. Parker, GBT Archive A0325
- [12] NIST Technical Note 1297; Guidelines for Evaluating and Expressing the Uncertainty of NIST Measurement Results; Taylor and Kuyatt, 1994, available at <http://physics.nist.gov/cuu/Uncertainty/>

## Appendix A

# Options and Methods for Weighing the GBT

## Appendix B

# Proposed Procedure for Weighing the GBT

## Appendix C

# Geokon Load Cell Manual

## Appendix D

# Pressure Gage Calibration Reports

## Appendix E

# Jack and Hydraulic Drawings

Appendix F

## Pre-weighing Calibration

## Appendix G

# Load Field Notes and Location Sketches

**Appendix H**

**Pointer Field Notes**

**Appendix I**

**Inclinometer Field Notes**

Appendix J

# Post-weighing Calibration

## Appendix K

# Force, Angle, and Excitation Plots

## Appendix L

# Force Tables—Load Cells

## Appendix M

# Force Tables—Hydraulic Jacks

Appendix N

Indicator Plots

# Appendix O

## CD

- O.1 Calibration Reports and Photos
- O.2 Excel files
- O.3 Photos
- O.4 T<sub>E</sub>XFiles
- O.5 Powerpoint File

<b>H</b>	<b>Pointer Field Notes</b>	<b>VIII</b>
<b>I</b>	<b>Inclinometer Field Notes</b>	<b>IX</b>
<b>J</b>	<b>Post-weighing Calibration</b>	<b>X</b>
<b>K</b>	<b>Force, Angle, and Excitation Plots</b>	<b>XI</b>
<b>L</b>	<b>Force Tables—Load Cells</b>	<b>XII</b>
<b>M</b>	<b>Force Tables—Hydraulic Jacks</b>	<b>XIII</b>
<b>N</b>	<b>Indicator Plots</b>	<b>XIV</b>
<b>O</b>	<b>CD</b>	<b>XV</b>
	O.1 Calibration Reports and Photos . . . . .	XV
	O.2 Excel files . . . . .	XV
	O.3 Photos . . . . .	XV
	O.4 T <sub>E</sub> XFiles . . . . .	XV
	O.5 Powerpoint File . . . . .	XV

# List of Figures

1.1	The Robert C. Byrd Green Bank Telescope. . . . .	2
1.2	Geokon 2,000 kip load cell. . . . .	2
2.1	Materials testing machine and platens. . . . .	5
2.2	Load cell centered on platens with aluminum plates. . . . .	5
2.3	Load cell between platens. . . . .	6
2.4	Alidade corner . . . . .	6
2.5	N3 Optical level . . . . .	8
2.6	Clineometer measurement of corner weldment . . . . .	9
2.7	Instrumentation truck. . . . .	9
2.8	End view of wiffle beam. . . . .	10
2.9	Initial load cell configuration. . . . .	10
2.10	Revised load cell configuration. . . . .	11
2.11	Inboard lifting fixture. . . . .	12
2.12	Hydraulic system. . . . .	13
2.13	Schedule of Operations. . . . .	13
2.14	Crew. . . . .	14
2.15	Load cell calibration with lead sheets. . . . .	15
3.1	Histogram of ascending $\Delta F/\Delta\alpha$ for load cells. . . . .	18
3.2	Histogram of descending $\Delta F/\Delta\alpha$ for load cells. . . . .	18
3.3	Histogram of ascending $\Delta F/\Delta\alpha$ for hydraulic pressure. . . . .	19
3.4	Histogram of descending $\Delta F/\Delta\alpha$ for hydraulic pressure. . . . .	19
3.5	Histograms of residual load cell force on cell 1976—including jack friction. . . . .	20
3.6	Histograms of residual load cell force on cell 2081—including jack friction. . . . .	20
3.7	Histograms of zero force on cell 1976. . . . .	21
3.8	Histograms of zero force on cell 2081. . . . .	21
3.9	Summary of GBT rolling weight. . . . .	22
4.1	Typical jack stroke measurement data . . . . .	25
4.2	Measurement of vertical motion between wheel housing and wiffle beam . . . . .	26
4.3	Vertical movement between wheel housing and wiffle beam—jacking beam. . . . .	27
4.4	Vertical movement between wheel housing and wiffle beam—idler beam. . . . .	27
4.5	Measurement of vertical motion between wheel housing and wiffle beam at both distal flex plates. . . . .	28
4.6	Measurement of vertical motion between wheel housing and wiffle beam at both proximal flex plates. . . . .	28
4.7	Measurement of horizontal deflection of wiffle beam. . . . .	29
4.8	Measurement of the compression of the top beams. . . . .	29
4.9	Flex plate length measurement. . . . .	30
4.10	Detail of flex plate length measurement. . . . .	31
4.11	Flex plate length data. . . . .	31
4.12	Idler circumferential measurement. . . . .	32
4.13	Idler wheel movement. . . . .	33